# Models of the Lunar Surface Including Temperature-Dependent Thermal Properties

JEFFREY L. LINSKY[1]

*Harvard College Observatory, Cambridge, Massachusetts*

The thermal conditions in the lunar surface are considered on a gross scale in terms of models with temperature-dependent thermal properties, including radiative energy transport. Agreement is obtained with infrared measurements of cold terminator temperatures and radio lunation data at millimeter wavelengths for a range of postulated parameters of the surface material. The observed increase of mean radio brightness temperature with wavelength is interpreted as due to radiative energy transport and the resultant non-linearity of the heat-conduction equation, rather than to a large radioactive heat flux.

The postulated existence of radiative energy transport is consistent with a porous or frothy medium, in agreement with photometric and laboratory simulation experiments, as well as with recent radar depolarization measurements. A distance scale of 0.1–0.3 mm for the effective mean separation of radiating surfaces is suggested by this interpretation of the data.

## I. Introduction

At the present time contradictions exist between deduced thermal properties of the lunar surface as interpreted from infrared and from radio observations. In addition, high-precision radio observations have been interpreted in terms of an unexpectedly large thermal flux in the lunar surface material.

In this paper I suggest a means whereby these contradictions may be resolved by considering temperature dependence of the conductivity, including a radiative contribution, and of the specific heat. I have written a computer program to solve the heat-conduction equation for arbitrary temperature- and depth-dependent thermal properties during a lunation and an eclipse, and to compute radio brightness temperatures for such models of the lunar surface.

It is first shown that the mean temperature beneath the surface increases significantly with depth for no net thermal flux

[1] Present address: Smithsonian Astrophysical Observatory, Cambridge, Massachusetts.

only if the conductivity increases with temperature. Recent measurements of postulated lunar materials indicate such a temperature dependence. Therefore, an observed increase of the mean radio brightness temperature with wavelength may be indicative of the thermal properties of the material and not of the net thermal flux resulting from radioactive heating.

Secondly, it is argued that radio measurements cannot be interpreted uniquely in that two parameters are involved in an ambiguous manner, i.e., the ratio of the thermal to the electromagnetic wavelengths and a product of thermal properties. The radio data may, therefore, be reinterpreted in terms of models suggested by recent infrared measurements of the minimum surface temperature reached during the lunar night.

Each of eight simple models, six of which have temperature-dependent thermal properties, agrees well with infrared eclipse and lunation data as well as with radio observations in the millimeter range. All but one are

homogeneous with depth to at least several meters and are stratified although a more complex structure is probably more realistic. This group of models suggests that the surface layer may be a highly porous, possibly frothy, one in which radiation plays a significant role in heat transfer in the material. Such a tentative model is in agreement with recent radar depolarization data and laboratory simulation experiments.

It should be emphasized that the actual lunar surface may be quite complicated, consisting of many materials arranged in depth and across the surface. This picture is suggested by recent high resolution infrared, radio, and radar data. This paper is an attempt to describe the gross thermal properties of a region of the lunar surface, the subterrestrial region, so as to be consistent with recent infrared, radio, and radar data, by means of simple models incorporating temperature-dependent thermal properties. The approach should give information about this region if the actual inhomogeneities act only as fine structure upon the emitted thermal radiation rather than as important contributions to this radiation. If the contrary proves to be true, which is the more likely case, then the present methodology should be valid provided one weighs the contributions to the infrared and radio signals by the relative proportions of the various materials in the field of view. As the data become more numerous, such an approach becomes more fruitful and should be pursued.

## II. PREVIOUS INTERPRETATIONS OF INFRARED AND RADIO OBSERVATIONS

The first attempts at characterizing the thermal properties of the lunar surface consisted of solutions to the heat-conduction equation in a homogeneous, plane-parallel medium of temperature-independent properties under boundary conditions appropriate for a lunation and an eclipse. Wesselink (1948) obtained reasonable agreement between his theoretical eclipse cooling curves and Pettit's (1940) eclipse data for a model in which the thermal parameter

$$\gamma = (\kappa \rho c)^{-\frac{1}{2}} \approx 1000 \text{ cm}^2 \text{ °K cal}^{-1} \text{ sec}^{-\frac{1}{2}},$$

where $\kappa$ is the thermal conductivity; $\rho$, the density; and $c$, the specific heat. Jaeger and Harper (1950) and some subsequent investigators have obtained better agreement with two-layer models.

Prior to 1962 the only temperature measurement of the dark side of the Moon available was the value of $120° \pm 15°$K obtained by Pettit and Nicholson (1930), later confirmed by Sinton (1962). Jaeger (1953) found this midnight temperature consistent with a homogeneous model with $\gamma \approx 500$, or by two-layer models consisting of less than a centimeter of insulating materials over a more conducting medium. With the vast improvement of infrared instrumentation—and especially the recent measurements by Low (1965)—the mean temperature of the cold lunar limb has been more reliably established at 90°K. Thus both eclipse and lunation infrared measurements may be explained in terms of a typical lunar surface element homogeneous at least to a depth of centimeters, several thermal wavelengths, and characterized by $\gamma \approx 1000$.

In the last five years important observations at millimeter and centimeter wavelengths have been made in the Soviet Union by Salomanovich, Troitsky, Kislyakov, and many others. Krotikov and Troitsky (1963) have summarized this work. Within the confines of a linear theory, e.g., one in which the thermal and electromagnetic properties are assumed to be temperature-independent, these data have been interpreted in terms of a homogeneous lunar surface to a depth of several meters, characterized by $\gamma \approx 350$ as opposed to the value of 1000 suggested by the infrared data. Their interpretation of these data apparently is inconsistent with a thin layer of highly insulating material covering a large fraction of the lunar surface, which would exhibit the rapid surface cooling observed in the infrared during an eclipse and during the lunar night.

A further important result of this work is an apparent measurement of the thermal gradient in the lunar surface. Krotikov and Troitsky (1963, 1964) have interpreted the observed increase in the mean brightness temperature as measured by several radio-telescopes using the "artificial Moon" cali-

bration procedure (see Krotikov, Porfiryev, and Troitsky, 1961) in terms of a heat flux produced by a level of radioactivity four to six times in excess of that predicted by MacDonald (1959), Levin and Maeva (1961), and Jaeger (1959) under the assumption of chondritic lunar material. However, the measured thermal gradient, as Krotikov and Troitsky have shown, produces a temperature $\approx 1000°K$ at a depth of 60 km and may well lead to a molten lunar interior, if the Moon consists in large part of this material. The observed nonspherical shape of the Moon makes the possibility of a molten interior highly questionable.

Thus, recent infrared and radio observations, when interpreted in terms of temperature-independent thermal properties for the lunar surface material, lead to contradictory and disturbing conclusions. To explain the contradiction between infrared and radio observations, one must show that either one or both sets of observations has been interpreted incorrectly; or, there must be a mechanism whereby the lunar material can exhibit more insulating properties ($\gamma$ large) at the surface during lunar nighttime, while at the same time the material exhibits a significantly smaller thermal parameter at centimeter and meter depths beneath the surface, where the observed radio emission originates. Thus, near the surface during the lunar night, the product of $\kappa\rho c$ must be an order of magnitude smaller than a few centimeters or meters beneath the surface. Yet at the same time, the radio data apparently do not allow the surface material to exhibit different thermal properties *on the average* over a lunation from the material directly below it. Thus, an increase with temperature of the thermal conductivity and the specific heat are expected. This tentative conclusion has also been suggested by Krotikov and Troitsky (1963) and Muncy (1958, 1963). Prior to this time, models of the lunar surface including temperature-dependent properties have been computed for special cases by Wesselink (1948), Muncey (1958, 1963), Watson (1964), Tyler (1961), and by Tyler and Copeland (1962).

## III. MEASUREMENTS AND LIKELY THERMAL PROPERTIES OF POSTULATED LUNAR SURFACE MATERIALS

The specific heats of many silicates, oxides, and terrestrial rocks have been measured in the laboratory in the temperature range of 70°–400°K. All of these materials described in Goldsmith, Waterman, and Hirschhorn (1958) exhibit a steep rise in thermal conductivity at low temperatures and then a gradual increase past 200°K to typical values of 0.18–0.24 cal gm$^{-1}$°K$^{-1}$ at 350°K. Buettner (1963) compared the specific heats of many such materials and concluded that in the lunar range of temperatures $c \sim T^{1/3}$, and thus a temperature-independent specific heat approximation may be justified.

Studies of the photometric and thermal properties of the lunar surface have suggested the basic picture of porous or finely divided "dust" materials in which there are relatively few contact points among the solid particles. In such a class of materials the thermal conductivity will be less— probably orders of magnitude less—than the conductivity of the same material as a solid, and radiative transport of energy in the material may play an important role. In order to obtain insight into the manner in which these two modes of energy transport may enter into the effective thermal conductivity, one can consider a number of idealized models of the lunar surface material microstructure.

In the first model (Case A in Fig. 1) I consider a very fragile structure, consisting of cubical cells of dimension $s$, in which no heat is transported along the thin opaque walls, and the thermal flux is carried only by radiation between them. In this case the thermal flux in direction $x$ is given by

$$F(x,T) = \epsilon_{IR}\sigma T^4(x) - \epsilon_{IR}\sigma T^4(x + s)$$

and the conductivity is purely radiative

$$\kappa_R(x,T) = 4\epsilon_{IR}\sigma T^3(x)s. \qquad (1)$$

In these equations $\epsilon_{IR}$ is the emissivity of the material, corrected for multiple reflections, corresponding to the peak of the Planck
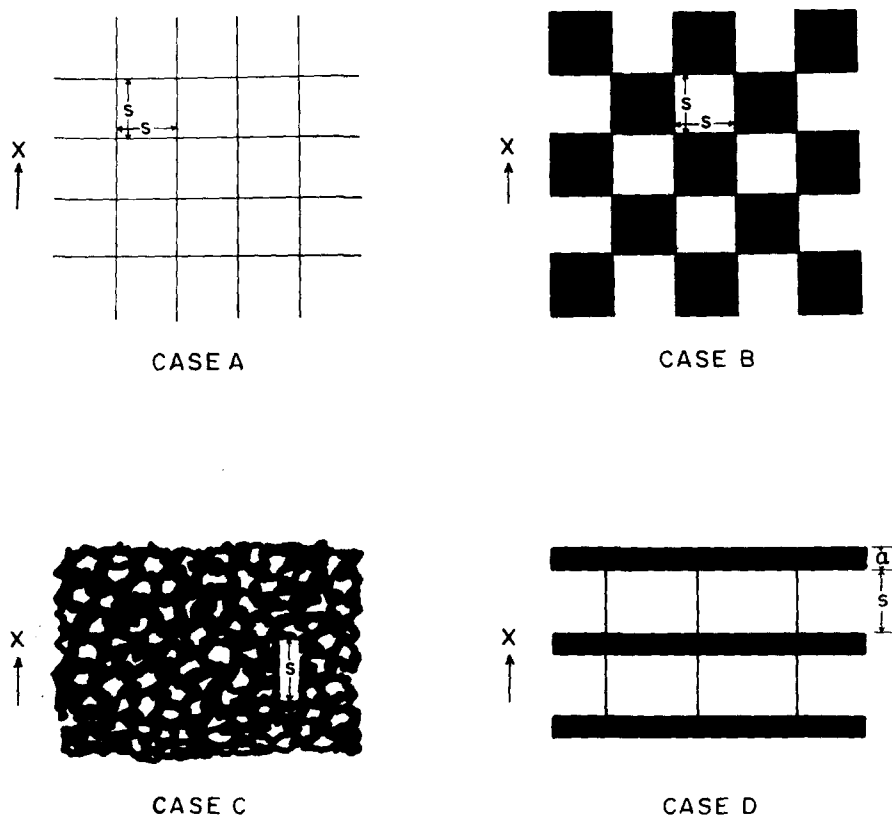
FIG. 1. Idealized models of the lunar surface microstructure in two-dimensional projection. Case A represents a structure in which the opaque walls are too thin to support appreciable thermal conduction so that the flux is carried by radiation alone. In Case B and Case C the flux is carried by conduction and by radiation in parallel, except that in the former example the solid material is opaque and in the latter it is partially transparent. Case D is an example of conduction and radiation in series.

spectral energy distribution at a temperature $T$, and $\sigma$ is the Stefan-Boltzmann constant.

In Case B, I consider an idealized cubical "grainy" structure where the flux is carried by conduction in the grains and radiation between them, but little or no flux is conducted at the contact points. In this situation, for any flux to be transported at all, radiation must play a role in tending to equalize the temperatures on the upper and lower surfaces of each cell. Therefore, the effective conductivity will be a linear combination of a purely conductive and a purely radiative component

$$\kappa(x,T) = \kappa_R(x,T) + \kappa_c(x). \qquad (2)$$

The purely conductive component of the conductivity will be controlled by the size of the contact "points" and thus can be orders of magnitude smaller than if the same material were a solid.

If we consider the opposite case of a porous medium in which the solid constituent is partly transparent to infrared radiation, depicted as Case C, then the flux is carried in parallel by conduction and the radiation field, and the effective flux is again a linear combination of the two components. Now, however, the radiation scale length $s$ is a measure of an infrared photon mean-free path for absorption and not of the geometrical microstructure of the material. In a more complex medium consisting of transparent and opaque materials, Eq. (2) may not be obeyed, but until evidence to the contrary is obtained, one would expect the

linear relationship of Eq. (2). Given this relationship, one can characterize the relative importance of the two components by their ratio at a specified temperature taken here to be 350°K

$$R_{350} = \kappa_R/\kappa_c = 4\epsilon_{IR}\sigma(350)^3s/\kappa_c.$$

There is, however, an idealized microstructure, albeit unlikely, in which Eq. (2) cannot be obeyed. This example, shown as Case D, is of a material in which the flux is carried by radiation and by conduction in series rather than in parallel. Conserving flux in the opaque solid material and the spaces in between, one obtains,

$$\kappa(T) = \left(\frac{a+s}{s}\right)\kappa_c$$
$$\times \left[\frac{R_{350}[a/(a+s)](T/350)^3}{1+R_{350}[a/(a+s)](T/350)^3}\right]. \quad (3)$$

The gross anisotropy of this model renders it unlikely.

Few measurements exist of thermal conductivities over the temperature range 100–400°K of finely ground silicates deposited under high vacuum conditions. Bernett, Wood, Jaffe, and Martens (1963) obtained thermal conductivities for several particle-size distributions of crushed olivine basalt in the range 4–15 $\times$ 10$^{-6}$ cal cm$^{-1}$ sec$^{-1}$ °K$^{-1}$ between $-70°$ and $+90°$C. Measurements for each sample tended to increase with temperature, but the one sample ($-35$ mesh, $\rho = 1.49$ gm cm$^{-3}$) that exhibited the greatest temperature variation can be characterized in the temperature range $-10°$ to $+90°$C by $\kappa_c = 2.2 \times 10^{-6}$ and $R_{350} \simeq 2$.

Buettner (1963) describes measurements performed on crushed basalt powder of 5$\mu$ grain size that can be characterized by $\kappa_c \simeq$ 9 $\times$ 10$^{-6}$ and $R_{350°K} \simeq 2.5$. These and subsequent data are summarized in Table I.

Watson (1964) has measured the thermal conductivities of dry powdered silicates at 10$^{-5}$ to 10$^{-6}$ torr between 150° and 350°K. His data are well described by the functional form (2) with the radiative and conductive terms a function of particle size. In particular, the conductive component was found to be independent of composition and inversely proportional to particle size. The radiative component consisted of a constant term corresponding to transmission through small grains and a term linear in particle size corresponding to radiation between large particles.

More recently Wechsler and Glaser (1965) have summarized the measurements of the thermal conductivities of porous rocks and powders. The data for rock powders measured at pressures near 10$^{-5}$ torr fall in the range of 5 $\times$ 10$^{-6}$ < $\kappa(T)$ < 10 $\times$ 10$^{-6}$ cal cm$^{-1}$ sec$^{-1}$ °K$^{-1}$. They cite thermal conductivity measurements that increase 30% for solid pumice (between 223° and 323°K), 50% for basalt lava (between 220° and 265°K), and 30% for basalt powder (between 221° and 331°K). Their first preliminary data on basalt powder (104–150 $\mu$ particle size) at the high vacuums of 5 $\times$ 10$^{-10}$ torr exhibit a very significant increase of 40–50% between 280° and 330°K. In this temperature range $\kappa_c \simeq 6 \times 10^{-7}$ and $R_{350} \simeq$ 10, but the data are widely scattered and $R_{350}$ may not be well determined.

TABLE I

SUMMARY OF RELEVANT MEASUREMENTS OF THE THERMAL PROPERTIES OF POSTULATED
LUNAR MATERIALS

| | $\rho$ (gm cm$^{-3}$) | Grain size (microns) | $\kappa_{350°K}$ (10$^{-6}$ cal cm$^{-1}$ °K$^{-1}$ sec$^{-1}$) | $\kappa_c$ | $R_{350}$ |
|---|---|---|---|---|---|
| Bernett *et al.* (1963) | 1.49 | 20–200 | 6.6 | 2.2 | 2. |
| Buettner (1963) | 2.61 | 5 | 31. | 9.0 | 2.5 |
| Watson (1964) | 1.50 | 30 | 4.3 | 1.4 | 2. |
| Watson (1964) | 1.50 | 100 | 6.7 | 0.67 | 9. |
| Watson (1964) | 1.50 | 300 | 14. | 0.24 | 57. |
| Wechsler & Glaser (1965) | — | 104–150 | 6.6 | 0.6 | 10. |
| For $\gamma = 1000$, $c = 0.2$ | 1.00 | 0 | 5.0 | 5.0 | 0 |
| For $\gamma = 350$, $c = 0.2$ | 1.00 | 0 | 41. | 41. | 0 |

These data as summarized in Table I are far from conclusive, but they do make it imperative that radiative conductivity be considered. Unfortunately, other effects such as possible changes in density, adhesion, or contact resistance with temperature may be important and may affect the thermal properties. For this reason I have calculated models also for a general power law approximation to the conductivity over the lunar range of temperatures

$$\kappa(x,T) = \kappa_0(x)T^a. \qquad (4)$$

## IV. COMPUTATIONAL PROCEDURES

Computations are described of the surface temperature $T(0,t)$ and internal temperature distribution $T(x,t)$ during a lunation and an eclipse in a plane-parallel medium in which the thermal and electromagnetic properties are assumed only to be a function of depth $x$ beneath the surface. The surface material has been assumed opaque in the middle infrared (5–40 $\mu$), as suggested by Launer (1952), but partially transparent in the radio region. The heat-conduction equation

$$\rho c(x,T) \frac{\partial T(x,t)}{\partial t} = \frac{\partial}{\partial x}\left[ \kappa(x,T) \frac{\partial T(x,t)}{\partial x} \right], \quad (5)$$

subject to boundary conditions

$$\left[ \kappa(x,T) \frac{\partial T(x,t)}{\partial x} \right]_{x=0} = \epsilon_{IR}\sigma T^4(0,t)$$
$$- \epsilon_B I(\xi,\eta,t), \quad (6)$$

and

$$T(x,t) = \text{constant as } x \to \text{large}, \quad (7)$$

is solved by difference equation techniques on an IBM 7094 computer. In Eqs. (5), (6), and (7) we define $\epsilon_{IR}$ as the mean emissivity at the wavelengths corresponding to the peak of the Planck distribution at lunar temperatures; $\epsilon_B$, as the bolometric emissivity for solar illumination; and $I(\xi,\eta,t)$, as the insulation at lunar rectangular coordinates $(\xi,\eta)$, and time $t$.

The complete difference equations and the method of their solution are fully described in Ingrao, Young, and Linsky (1965) and Linsky (1965). All of these computations were made for 20 discrete depths between

the surface and a depth of 4 or 5 thermal wavelengths, and for at least 4000 times during a lunation. Care was taken to damp out errors in the assumed initial temperature distributions, so that the internal temperature distributions should be correct to $\pm 1°K$, at least to a depth of one thermal wavelength.

Computations have been performed for three different representations of the thermal properties in order to determine the effects of nonlinearities in the heat-conduction equation upon the observable thermal emission.

*Model Type I*—Temperature-independent thermal properties

$$\kappa(x,T) = \kappa(x)$$
$$c(x,T) = c(x)$$
$$\gamma_c(x) = \gamma_{350}(x) = [\kappa(x)\rho(x)c(x)]^{-1/2}$$

*Model Type II*—Radiative and thermal conductivity

$$\kappa(x,T) = \kappa_c(x) + 4\epsilon_{IR}\sigma T^3(x,t)s(x)$$
$$c(x,T) = c(x)T^b(x,t)$$
$$\gamma_c(x) = [\kappa_c(x)\rho(x)c(x,350°K)]^{-1/2}$$
$$\gamma_{350}(x) = [\kappa(x,350°K)\rho(x)c(x,350°K)]^{-1/2}$$

*Model Type III*—Power law approximation to the thermal properties

$$\kappa(x,T) = \kappa_0(x)T^a(x,t)$$
$$c(x,T) = c_0(x)T^b(x,t)$$
$$\gamma_{350}(x) = [\kappa(x,350°K)\rho(x)c(x,350°K)]^{-1/2}.$$

Solutions of the heat-conduction equation in homogeneous media are most easily expressed as functions of the thermal parameter $\gamma$, when the depth variable is expressed in units of the thermal wavelength,

$$l_{1T} = P\kappa/(\pi\rho c)^{1/2}, \qquad (8)$$

the depth at which the amplitude of the first harmonic in a Fourier expansion of $T(x,t)$ is reduced to $e^{-1}$ of its surface amplitude. Here $P$ is the lunar synodic period. (See Wesselink, 1948 and Carslaw and Jaeger, 1959.) However, if one wishes to consider a multilayer model, it is often more convenient to consider the physical depth $x$ as the independent variable. In this representa-

tion, solutions of the heat-conduction equations are functions of the diffusivity $\alpha$

$$\alpha = \kappa/\rho c. \tag{9}$$

For each model computed, the specific heat has been assumed to be 0.20 cal gm$^{-1}$ °K$^{-1}$ or this value at 350°K when temperature-dependent, and unless specified, the density has been assumed to be 1 gm cm$^{-3}$. Thus one needs only to specify $\kappa(x,T)$ for each model and one may characterize each in more familiar terms by the value of $\gamma_{350}(x) = [\kappa(x,350°K)\rho(x)c(x,350°K)]$. Each solution will be invariant to multiplying $\kappa$ and $\rho$ by a constant factor with $\gamma_{350}$ being reduced by that factor.

For these calculations, a value of 0.88 has been assumed for $\epsilon_B$ and $\epsilon_{IR}$. The former value has been estimated from the albedo data cited in Harris (1961) while the latter is in agreement with measurements of 40 and 400 $\mu$ quartz sand by Burns and Lyon (1963) and measurements of assumed lunar powders in the 7–14 $\mu$ wavelength region by Van Tassel and Simon (1964). Krotikov and Shchuko (1963) have shown that the nighttime surface temperatures, which most conclusively differentiate one model of the surface from another, depend only very weakly upon $\epsilon_B$ and $\epsilon_{IR}$ for models with temperature-independent properties, and the same is true for the models under consideration. In agreement with Allen (1963), I have assumed a value of the solar constant of 1.99 cal cm$^{-2}$ min$^{-1}$, corresponding to a nonrotating blackbody equilibrium temperature of 395°K at 1 a.u. Deviations from a circular orbit considered by Tyler (1961) are of secondary importance and have not been taken into account.

Infrared brightness temperatures characterize the radiation from a grey surface of emissivity $\epsilon_{IR}$ as observed through a wide-band 8–14 $\mu$ filter. The procedure for deriving these quantities is described in Ingrao, Young, and Linsky (1965). These brightness temperatures will be subject to small corrections if the lunar spectral emissivity is not constant in the 8–14 $\mu$ region, as Burns and Lyon (1962) suggest, but they will vary significantly only at high temperatures for changes in the effective $\epsilon_{IR}$. The angular dependence of $\epsilon_{IR}$, as measured by Geoffrion, Korner, and Sinton (1960), and a possible transparency of the surface material in the infrared region, as discussed by Buettner (1963), have not been considered.

If one assumes homogeneous electromagnetic properties, e.g., no significant change in porosity or chemical composition with depth, and no scattering of thermal radiation at radio wavelengths in the medium or at the surface, the radio brightness temperature $T_R(\lambda,t)$ for wavelength $\lambda$ in the Rayleigh-Jeans approximation, shown by Piddington and Minnett (1949), is

$$T_R(\lambda,t) = (1 - R) \int_0^\infty T(x,t)$$
$$\times \exp(-k_\lambda x \sec\theta_{in})k_\lambda \sec\theta_{in}\, dx. \tag{10}$$

Here $R$ is the surface reflectivity; $k_\lambda$, the electromagnetic absorption coefficient at the observed wavelength $\lambda$; and $\theta_{in}$, the angle with respect to the normal made by an observed ray when in the medium. The method of evaluating Eq. (10) numerically will be described below.

In a dielectric, $k_\lambda$ will be of the form

$$k_\lambda = k_0/\lambda, \tag{11}$$

but if lattice vibrations are important, as Sinton (1962) suggests at the short millimeter wavelengths, this relation will not be valid. A value for $R$ may be obtained either from the dielectric constant and the Fresnel laws or from radar measurements. For these computations $R$ is assumed to be 0.05 at the center of the disk corresponding to a dielectric constant of 2.5, in close agreement with the values of 2.8 based on radar measurements of Evans and Pettengill (1963) and Rea, Hetherington, and Mifflin (1964). If the dielectric constant of the surface material is as low as 1.5, as suggested in Krotikov and Troitsky (1963) or in the range 1.7 to 1.8 according to Hagfors et al. (1965), then $R \simeq 0.01$ or 0.02, respectively, and all computed radio brightness temperatures should be increased.

For the computation of eclipse and lunation surface temperatures, it is not important to know accurately temperatures at depths in excess of a few thermal wavelengths. However, in the radio region of the spectrum

one may be observing radiation emitted from depths on the order of 10 or more times $\lambda$, and thus one must know temperatures at depths in the order of meters. The value of $T(x,t)$ more than a few centimeters beneath the surface will be independent of time and may be easily computed, assuming temperature-independent thermal properties, from the average value of the surface temperature over a lunation and an assumed mean thermal flux. In the general case of temperature-dependent properties, the determination of $T(x,t)$ beneath the surface is more complex.

## V. Variation of Average Temperature with Depth in the Lunar Surface

The heat-conduction equation (5), may be written in the form

$$\partial Q(x,t)/\partial t = \partial F(x,t)/\partial x, \qquad (12)$$

where $F(x,t)$ is the thermal flux

$$F(x,t) = \kappa(x,T)[\partial T(x,t)/\partial x], \qquad (13)$$

and $Q(x,t)$ is the heat content per unit volume of the material

$$Q(x,t) = \int_0^{T(x,t)} \rho(x)c(x,T)\, dT. \qquad (14)$$

Taking the time average of both sides of Eq. (12) over a lunation of synodic period $P$, one obtains

$$\frac{1}{P}\int_0^P \frac{\partial Q(x,t)}{\partial t}\, dt = \frac{1}{P}\int_0^P \frac{\partial F(x,t)}{\partial x}\, dt. \qquad (15)$$

The left-hand side of this equation may also be written as

$$\frac{\partial}{\partial t}\langle Q(x,t)\rangle = \frac{1}{P}\int_0^P \frac{\partial Q(x,t)}{\partial t}\, dt, \qquad (16)$$

where the symbol $\langle\ \rangle$ means time average over a lunation. Since the solar constant and presumably any internal heat sources in the lunar surface show no secular variation, and the Moon never deviates far from 1 a.u. from the Sun, $\partial\langle Q(x,t)\rangle/\partial t$ must be zero. Therefore,

$$\frac{\partial}{\partial x}\left\langle \kappa(x,T)\frac{\partial T(x,t)}{\partial x}\right\rangle = 0, \qquad (17)$$

and

$$\langle \kappa(x,T)[\partial T(x,t)/\partial x]\rangle = \langle F(x,t)\rangle = \text{constant}. \qquad (18)$$

In the special case of no internal heat sources and therefore no net thermal flux, this constant will be zero. Thus, for a stratified medium in which the thermal conductivity is depth-dependent but not a function of temperature,

$$\langle T(x,t)\rangle = \langle T(x=0,t)\rangle \quad \text{if} \quad \langle F(x,t)\rangle = 0$$

$$= \langle T(x=0,t)\rangle + \langle F(x,t)\rangle\int_0^x \frac{dx'}{\kappa(x')}$$

$$\text{if} \quad \langle F(x,t)\rangle \neq 0. \quad (19)$$

However, if the thermal conductivity is temperature-dependent, the mean value of the temperature may increase or decrease with depth even if $\langle F(x,t)\rangle$ is zero. This fact has been noted by Muncey (1958) and Krotikov and Troitsky (1963). For $\langle F(x,t)\rangle = 0$, and assuming

$$\kappa(x,T) = \kappa_0(x)T^a(x,t), \qquad (20)$$

one obtains

$$\langle T^{a+1}(x,t)\rangle = \text{constant} = \langle T^{a+1}(x=0,t)\rangle$$
$$\text{if} \quad a \neq -1,$$
$$\qquad (21)$$

or

$$\langle \log[T(x,t)]\rangle = \text{constant}$$
$$= \langle \log[T(x=0,t)]\rangle \text{ if} \quad a = -1.$$

Now one writes $T(x,t)$ as a Fourier series at each depth

$$T(x,t) = T_0(x) + \sum_{n=1}^{\infty} T_n(x)$$
$$\times \cos[n\omega t - \phi_n(x)], \quad (22)$$

where $T_n(x)$ and $\phi_n(x)$ are the amplitudes and phase lags relative to insolation, and $\omega = 2\pi/P$ is the lunar angular frequency of apparent rotation. Substituting Eq. (22) into (21), one obtains for integral positive values of $a$

$$T_0{}^2(x) = \langle T^2(x,t)\rangle - \frac{1}{2}\sum_{n=1}^{\infty} T_n{}^2(x)$$
$$\text{if} \quad a = 1, \quad (23a)$$

$$T_0{}^3(x) = \langle T^3(x,t) \rangle - \frac{3T_0(x)}{2} \sum_{n=1}^{\infty} T_n{}^2(x)$$
$$\text{if} \quad a = 2 \quad (23b)$$

and for nonintegral positive values the infinite series

$$T_0{}^{a+1}(x) = \langle T^{a+1}(x,t) \rangle - \frac{a(a+1)}{4} T_0{}^{a-1}(x)$$
$$\times \sum_{n=1}^{\infty} T_n{}^2(x) + \ldots \quad \text{if} \quad a > 0. \quad (23c)$$

Since the amplitudes $T_n(x)$ are real and decrease monotonically with depth and since the first term on the right-hand side of each equation is a constant, Eqs. (23a), (23b), and (23c) all exhibit solutions in which the average temperature $T_0(x)$ increases with depth, asymptotically approaching a limiting value that depends on this constant. This behavior is exhibited in Fig. 2 where the increase in $T_0(x)$ is given by $\Delta T = T_0$ (asymptotic) $- T_0(x = 0)$.

This increase in the average temperature with depth in the absence of internal heat sources can also be explained in terms of the following physical argument. To conserve flux at each depth over a lunation, as much heat must be conducted inward at this depth during the lunar day, as is conducted outward during the lunar night. By lunar night and day I mean those parts of a lunation in which the thermal gradient is negative and positive, respectively, at the depth under consideration. When the conductivity is temperature-independent, but not necessarily depth-independent, flux conservation requires the mean thermal gradients during day and night to be equal but of opposite sign. Thus the average temperature must be independent of depth.

However, when the conductivity depends upon temperature, the mean gradients during the day and night cannot be equal. In particular, if the conductivity is proportional to $T^3$, then flux conservation requires that the average value of $T^3$ times the temperature gradient during the day be cancelled by the same quantity during the night. Therefore, during the day the temperature gradient is small and negative, but during

the night it must be large and positive. The average gradient is thus positive and the average temperature increases with depth. This effect becomes more pronounced near the surface, where the amplitude of temperature variations is large, as is described by Eq. (23).

According to this argument, when the thermal conductivity decreases with temperature, the average temperature must decrease with depth

$$\log_e [T_0(x)] = \langle \log_e [T(x,t)] \rangle$$
$$+ \frac{1}{4} \sum_{n=1}^{\infty} \frac{T_n{}^2(x)}{T_0{}^2(x)} \quad \text{if} \quad a = -1, \quad (24a)$$

and

$$T_0{}^{-a+1}(x) = \langle T^{-a+1}(x,t) \rangle + \frac{a(1-a)}{4}$$
$$\times \sum_{n=1}^{\infty} \frac{T_n{}^2(x)}{T_0{}^{a+1}(x)} \quad \text{if} \quad a \neq -1,$$
$$a < 0 \quad (24b)$$
$$+ \ldots.$$

Now $T_0(x)$ decreases with depth approaching limiting values as shown in Fig. 2. For a two-term expression

$$\kappa(x,T) = \kappa_c(x) + \kappa_0(x) T^a(x,t),$$

similar formulas with similar dependencies upon depth may be obtained. In particular, for $a = 1$

$$T_0(x) = \langle T(x,t) \rangle + \frac{\kappa_0(x)}{2\kappa_c(x)} \langle T^2(x,t) \rangle$$
$$- \frac{1}{2} \left[ T_0{}^2(x) + \sum_{n=1}^{\infty} \frac{T_n{}^2(x)}{2} \right]. \quad (25)$$

When $\langle F(x,t) \rangle$ is not zero, a further increase of $T_0(x)$ with $x$ is superimposed upon the previous curves. For example, if $a$ is positive and

$$\kappa(x,T) = \kappa_0(x) T^a(x,t),$$

the analog of Eq. (21) contains an additional term

$$\langle T^{a+1}(x,t) \rangle = (a+1)\langle F(x,t) \rangle \int_0^x \frac{dx'}{\kappa_0(x')}$$
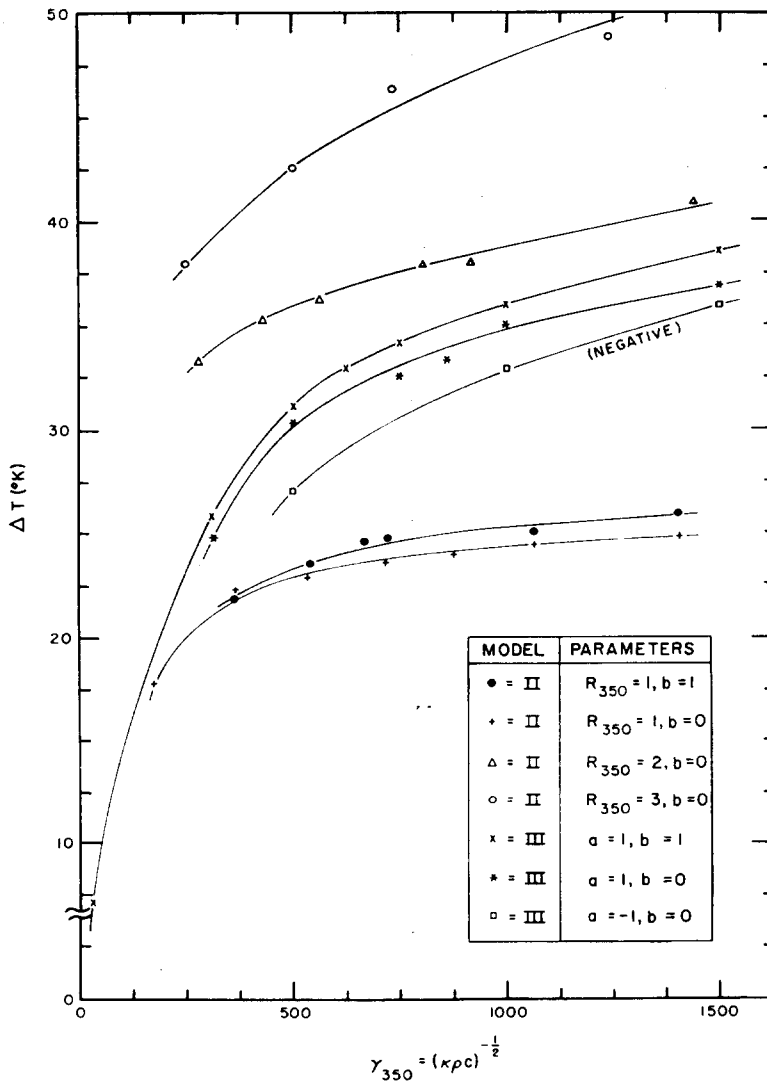$$+ \langle T^{a+1}(x = 0,t) \rangle, \quad (26)$$

FIG. 2. The difference $\Delta T$ between mean surface temperature and the asymptotic value of temperature beneath the surface, assuming no net thermal flux, plotted as a function of thermal parameter $\gamma_{350}$ defined at 350°K. Model Type II includes radiative conductivity, and Model Type III includes a general power law approximation to the temperature dependence of thermal conductivity and specific heat. $\Delta T$ is solely a result of nonlinearity introduced into the heat-conduction equation and is zero when thermal properties of the medium are assumed to be temperature-independent.

and now the general solution of Eq. (23c) becomes

$$T_0{}^{a+1}(x) = (a + 1)\langle F(x,t)\rangle \int_0^x \frac{dx'}{\kappa_0(x')}$$

$$+ \langle T^{a+1}(x = 0,t)\rangle - \frac{a(a + 1)}{4}$$

$$\times T_0{}^{a-1}(x) \sum_{n=1}^{\infty} T_n{}^2(x) + \ldots \quad (27)$$

Thus to the previous solutions a depth dependence is added to $T_0(x)$ roughly proportional to $x^{[1/(a+1)]}$.

In the absence of internal heat sources, the difference between the mean value of the temperature at the surface and its asymptotic value, reached at that depth at which the temperature does not vary over a lunation, can be as large as 50°K. This temperature difference $\Delta T$ increases with the

value of $a$ and decreasing conductivity, but is practically independent of any temperature dependence of the specific heat.

In Fig. 2 curves are plotted of the temperature difference $\Delta T$, assuming $\langle F(x,t)\rangle$ is zero. As expected from Eq. (18), any temperature dependence of the specific heat plays an unimportant role,[1] whereas the ratio of radiative to conductive flux at 350°K, $R_{350}$, or the conductivity temperature exponent are the important parameters.

For two-layer models, $\Delta T$ is intermediate between that characterizing the upper and lower layer materials. When the upper layer depth is about one-third of $l_{1T}$, $\Delta T$ is the mean of that computed for each layer separately. For the present I will consider the thermal wavelength $l_{1T}$ for temperature-dependent models to be the value of $P\kappa/(\pi\rho c)^{1/2}$ at the mean surface temperature.

In the simplest case of temperature-independent thermal properties

$$\langle T(x,t)\rangle = \langle T(x = 0,t)\rangle + \langle F(x,t)\rangle \int_0^x \frac{dx'}{\kappa(x)}.$$
(28)

For $\langle F(x,t)\rangle = 2.5 \times 10^{-7}$ cal cm$^{-2}$ sec$^{-1}$, as suggested above, $\langle T(x,t)\rangle$ increases over a distance of $4l_{1T}$ by 0.9°K for $\gamma = 1000$ and 0.15°K for $\gamma = 350$. Similar small increases in $\langle T(x,t)\rangle$ characterize temperature-dependent models. Thus the curves of $\Delta T$ vs. $\gamma_{350}$ in Fig. 2 are essentially unmodified.

Therefore, in evaluating the integral in Eq. (10), one can assume $\langle F(x,t)\rangle = 0$ to a depth of $4l_{1T}$ and use the temperature distributions $T(x,t)$ computed by adjusting $T(x = 4l_{1T})$, the temperature at the deepest point considered, such that flux conservation is obeyed. Beyond this depth the temperature is independent of time. Assuming a constant thermal flux at these depths,

$$F = \langle F(x,t)\rangle,$$

[1] The statements in Krotikov and Troitsky (1963, 1964) that a temperature dependence of the specific heat can introduce a change in mean temperature with depth are not supported by computations for a model in which $a = 0$ and $b = 1$; and the above theoretical considerations do not allow for any such variation.

the temperature for Model Type III will be given by

$$T(x) = \left\{\langle T^{a+1}(x = 0,t)\rangle \\ + (a + 1)F \int_0^x \frac{dx'}{\kappa_0(x')}\right\}^{1/(a+1)} \\ x > 4l_{1T} \quad (29)$$

and for Model Type II by the solution to the equation

$$T(x) + \frac{\sigma\epsilon_{IR}sT^4(x)}{\kappa_c(x)} = F \int_0^x \frac{dx'}{\kappa_c(x')} \\ + \langle T(x = 0,t)\rangle + \frac{\sigma\epsilon_{IR}s(x)}{\kappa_c(x)} \langle T^4(x = 0,t)\rangle \\ x > 4l_{1T}. \quad (30)$$

Radio brightness temperatures $T_R(\lambda,t)$ have been obtained by inserting computed values of $T(x,t)$ and $T(x)$ at large depths into Eq. (10) for the eight models consistent with infrared observations as described below. These radio temperatures evaluated at the subterrestrial point for 30 times during a lunation have been fitted to a three-term Fourier series,

$$T_R(\lambda,t) = T_{R0}(\lambda) + \sum_{n=1}^{3} T_{Rn}(\lambda) \\ \times \cos[n\omega t - \phi_n(x)], \quad (31)$$

using a least-squares procedure. The values of $T_{R0}(\lambda)$, $T_{R1}(\lambda)$, and $\phi_1(\lambda)$ are listed in Table II.

## VI. An Interpretation of Mean Radio Brightness Temperatures

Observations of the mean temperature of lunar thermal radiation cited by Krotikov and Troitsky (1963) were obtained with telescopes of low angular resolution compared to the lunar diameter. They have been modified by the correction procedure of Krotikov (1965) to be applicable to the center of the disk, assuming a dielectric constant of 2.5, and are plotted in Fig. 3 along with the values of $T_{R0}(\lambda)$ for the eight computed lunar surface models consistent with infrared lunation measurements. The effect of temperature-dependent thermal properties should not subject this modification procedure to systematic errors that

## TABLE II
### RADIO DATA AND COMPUTED MODELS

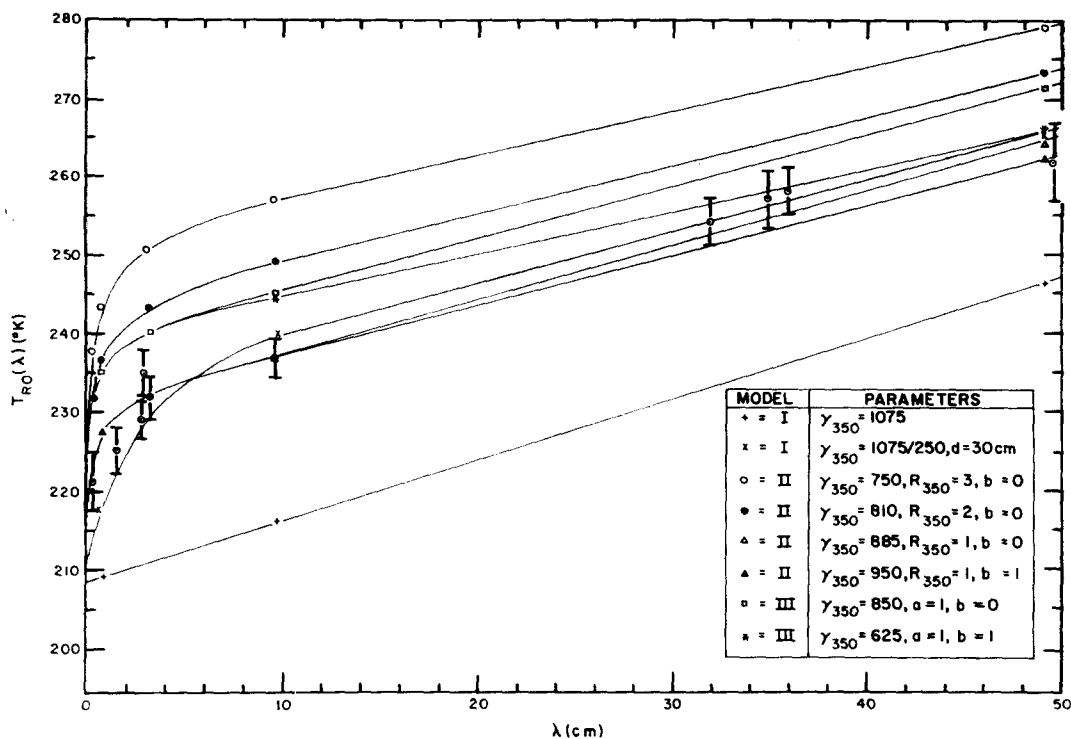| Model parameters | $T_{R0}$ (1.2 mm) (°K) | $T_{R0}$ (50 cm) (°K) | $k_0$ (cm$^{-1}$) | $\dfrac{T_{Ri}(1.2\ mm)}{T_{R0}(1.2\ mm)}$ | $\phi_1$ (1.2 mm) (deg) | $\dfrac{T_{Ri}(3.3\ mm)}{T_{R0}(3.3\ mm)}$ | $\phi_1$ (3.3 mm) (deg) | $\dfrac{T_{Ri}(4\ mm)}{T_{R0}(4\ mm)}$ | $\phi_1$ (4 mm) (deg) | $\dfrac{T_{Ri}(8\ mm)}{T_{R0}(8\ mm)}$ | $\phi_1$ (8 mm) (deg) | $\dfrac{T_{Ri}(3.2\ cm)}{T_{R0}(3.2\ cm)}$ | $\phi_1$ (3.2 cm) (deg) |
|---|---|---|---|---|---|---|---|---|---|---|---|---|---|
| I  $\gamma_c = 1075$ | 209.3 | 247.1 | 0.096 | 0.578 | 16.1 | 0.385 | 27.3 | 0.345 | 29.5 | 0.215 | 36.5 | 0.064 | 44.4 |
| I  $\gamma_c = 1075, \gamma_c = 250(z > 30$ cm$)$ <br> $((F) = 4.8 \times 10^{-6}$ cal cm$^{-2}$ sec$^{-1})$ | 210.8 | 266.9 | 0.096 | 0.572 | 16.1 | 0.379 | 27.3 | 0.341 | 29.5 | 0.210 | 36.5 | 0.064 | 44.5 |
| II  $\gamma_{380} = 885, R = 1, b = 0$ | 217.6 | 265.5 | 0.097 | 0.564 | 16.1 | 0.371 | 27.2 | 0.331 | 29.4 | 0.205 | 36.5 | 0.064 | 44.3 |
| II  $\gamma_{380} = 810, R = 2, b = 0$ | 221.5 | 274.0 | 0.101 | 0.556 | 15.4 | 0.365 | 26.3 | 0.327 | 28.4 | 0.203 | 35.5 | 0.060 | 43.4 |
| III  $\gamma_{380} = 750, R = 3, b = 0$ | 225.3 | 279.6 | 0.097 | 0.538 | 15.6 | 0.349 | 26.2 | 0.312 | 28.3 | 0.193 | 35.3 | 0.057 | 43.3 |
| III  $\gamma_{380} = 670, R = 1, b = 1$ | 217.8 | 263.0 | 0.062 | 0.568 | 16.2 | 0.374 | 27.3 | 0.335 | 29.7 | 0.207 | 36.7 | 0.061 | 44.5 |
| III  $\gamma_{380} = 850, a = 1, b = 0$ | 223.2 | 272.0 | 0.090 | 0.523 | 15.9 | 0.335 | 26.8 | 0.298 | 29.0 | 0.184 | 35.9 | 0.054 | 43.4 |
| III  $\gamma_{380} = 625, a = 1, b = 1$ | 222.8 | 266.4 | 0.062 | 0.538 | 15.4 | 0.355 | 26.0 | 0.318 | 28.3 | 0.198 | 35.2 | 0.059 | 43.4 |
| Observations (wavelength and beam width) | $T_{R0}(\lambda)$ | | | | | | | | | | | | |
| Low and Davidson (1965) 1.2 mm, 3'.9, 1'.0 | 229 | | | | | | | | | | | | |
| Fedoseyev (1963) 1.3 mm, 10' | 219 | | | 0.555 | 16 | | | | | | | | |
| Gary et al. (1965) 3.3 mm, 2'.9 | 196 | | | | | | | | | | | | |
| Kislyakov and Salomonovich (1963) 4 mm, 1'.6 | 228 | | | | | | | 0.377 | 27 | | | | |
| Salomonovich and Losovsky (1962) 8 mm, 2' | 211 | | | | | | | | | 0.189 | 30 | | |
| Kuschenko, Losovsky, and Salomonovich (1961) 3.2 cm, 6' | 223 | | | | | | | | | | | 0.076 | 45 |
| Mayer, McCullough, and Sloanaker (1961) 3.2 cm, 9' | 195 | | | | | | | | | | | 0.061 | 44 |

FIG. 3. Curves showing computed values of the mean component of radio brightness temperature at the center of the disk as a function of wavelength. Data points are those tabulated in Krotikov and Troitsky (1963), modified to correspond to center of disk by use of parameters computed by Krotikov (1965) and a dielectric constant of 2.5. Computed temperatures include surface reflectivity loss of 5%. Net thermal flux of $3.4 \times 10^{-7}$ cal cm$^{-2}$ sec$^{-1}$ has been assumed, for all models but one, so as to produce a rate of increase of radio brightness temperature between 3.2 and 50 cm commensurate with the data. A flux of $4.8 \times 10^{-6}$ cal cm$^{-2}$ sec$^{-1}$ was chosen for the two-layer model to satisfy the data between 0.4 and 3.2 cm, and the lower layer thermal parameter was chosen to produce the observed increase in temperature between 3.2 and 50 cm.

depend upon $\lambda$. For a dielectric constant of 1.8, all of these data points would be decreased by 1% and the computed radio temperatures increased by 3%. Except where noted, an internal flux of $3.4 \times 10^{-7}$ cal cm$^{-2}$ sec$^{-1}$ has been chosen to fit the observed rate of temperature increase at wavelengths longer than 3.2 cm.

Unfortunately, absolute flux measurements are indeed very difficult, and it is a credit to those who designed the "artificial Moon" method that it has been used. However, this procedure requires elaborate corrections for diffracted terrestrial radiation by the observed disk (see Tseytlin, 1963, 1964) and assumptions concerning the effective solid angle of interception of the disk's diffraction pattern by the Earth and its

relation to the diffraction correction.[2] Since the effects of deviations from these assumptions will depend upon the disk's diffraction pattern and therefore the observing wavelength, any systematic errors in this calibration procedure may be wavelength-dependent and modify my conclusions.

The simplest models that predict a dependence of $T_{R0}(\lambda)$ upon $\lambda$ consistent with the absolute mean temperature measurements in Fig. 2 are two radiative models ($\gamma_{350} = 885$, $R_{350} = 1$, $b = 0$) and ($\gamma_{350} = 670$, $R_{350} = 1$, $b = 1$); and the two-layer temperature-independent model ($\gamma_c = 1075$ upper layer 30 cm deep and $\gamma_c = 250$ lower layer). The parameters for the later model

[2] Note Eq. (10) in Tseytlin (1963).

were chosen to exhibit a steep rise in $T_{R0}(\lambda)$ between 1 and 3.2 cm and a less steep rise at larger wavelengths. If the dielectric constant is smaller than the assumed value of 2.5, one must modify the parameters in these three models to effect good agreement with the data. Choosing a dielectric constant of 1.5 as a plausible lower limit, I have interpolated among the computed models to obtain the estimated parameters shown in Table III.

The above analysis shows that under the assumption of temperature-independent thermal properties, only an increase of the conductivity with depth can account for the form of the mean radio brightness data shown in Fig. 2. No distribution of materials on the surface can produce other than a linear increase with wavelength. However, the mean thermal flux necessary to maintain the observed $T_{R0}(\lambda)$ for the two-layer models is from 15 to 23 times that predicted for

TABLE III
MODELS IN AGREEMENT WITH MEAN RADIO BRIGHTNESS DATA

| | Model parameters | | | $s$ (mm) | $\langle F(x,t)\rangle$ (cal cm$^2$ sec$^{-1}$) |
|---|---|---|---|---|---|
| | | $\epsilon = 2.5$ | | | |
| I | $\gamma_c = 1075$ | $\gamma_c = 250 (x > 30$ cm$)$ | | — | $4.8 \times 10^{-6}$ |
| II | $\gamma_{350} = 885$ | $R_{350} = 1$ | $b = 0$ | 0.16 | $3.4 \times 10^{-7}$ |
| II | $\gamma_{350} = 670$ | $R_{350} = 1$ | $b = 1$ | 0.27 | $3.4 \times 10^{-7}$ |
| | | $\epsilon = 1.5$ | | | |
| I | $\gamma_c = 1075$ | $\gamma_c = 460 (x > 30$ cm$)$ | | — | $3.3 \times 10^{-6}$ |
| II | $\gamma_{350} = 975$ | $R_{350} = 1/2$ | $b = 0$ | 0.08 | $3.4 \times 10^{-7}$ |
| II | $\gamma_{350} = 1030$ | $R_{350} = 1/2$ | $b = 1$ | 0.11 | $3.4 \times 10^{-7}$ |

From these parameters and the data one can place outer limits upon the deduced mean thermal flux passing through the surface material due to internal heat sources. Using the conductivities appropriate to the four radiative models described in Table III and a criterion of satisfying six of the eight data-point error brackets between 3.2 and 50 cm, I obtain a value of $2.7 \times 10^{-7}$ cal cm$^{-2}$ sec$^{-1}$ for the lower limit, and $4.2 \times 10^{-7}$ cal cm$^{-2}$ sec$^{-1}$ for the upper limit. Corresponding values of the flux for the two-layer models with temperature-independent properties are $3.7 \times 10^{-6}$ and $5.8 \times 10^{-6}$ cal cm$^{-2}$ sec$^{-1}$, respectively.

An alternative explanation of the increase in mean temperature with depth is that this is the thermal gradient between a hot interior and a cold surface. According to the interior models of MacDonald (1959) which exhibit the largest surface thermal gradient, typical values are 0.04°C/meter. These gradients are about three orders of magnitude lower than the radio data suggest and would lead to no measurable increase in the mean radio brightness temperature with wavelength.

chondritic materials. More radioactive materials do exist, but if meteoritic samples may be considered a guide, they are less common in the solar system. In addition, there is the problem of supporting the nonequilibrium figure of the Moon, which is aggravated by this high level of radioactive heating. Therefore, the radiative models appear to be the more plausible explanation of the data.

A further result of this analysis is an estimate of the distance scale of separation of radiating surfaces in the lunar material. This mean effective spacing would correspond to an average pore size in a porous medium or to an interparticular spacing in a grainy or dusty medium. Typical values of 0.1 to 0.3 are suggested in agreement with Wesselink's (1948) original estimate. If the lunar material is partially transparent to infrared radiation, these scale lengths set upper limits to the average pore size or interparticular spacing. This distance scale is an order of magnitude larger than that proposed by Hapke and Van Horn (1963) to account for the photometric properties of the lunar surface.

## VII. An Interpretation of Infrared Observations

In any attempt to understand the thermal behavior of the lunar surface material, one should consider each method of obtaining information in the light of its inherent limitations and the degree to which the fundamental data on the surface material parameters have been smeared out or convoluted with unwanted information. For the interpretation of radio data on the increase of brightness temperature with wavelength, one must compare absolute measurements that are affected by side lobes, telescope efficiency, and sky background, and the necessity of independent knowledge of the electromagnetic absorption coefficient $k_\lambda$. Radio observations of amplitudes and phase lags of Fourier components of the integrated lunar emission require relative measurements and are thus the more reliable.

Infrared data on the surface brightness temperature, by its very nature, must give the most reliable information of the thermal properties of the lunar surface material at small depths short of actual measurement *in situ*. Assuming that one is indeed observing the surface temperature of an opaque medium, this temperature is affected only by an emissivity factor that is unknown and may be temperature-dependent. However, in the 8–14 and 17–22 $\mu$ regions of the spectrum, one is observing during the lunar night in the Wien domain of the Planck spectral energy distribution, where the observed temperatures are very weakly affected by flux measurement errors and departures from a blackbody. For example, in the 8–14 $\mu$ window a 12% error in the measured flux or an emissivity of 0.88 produces only a 1°K error in deduced surface temperature for temperatures near 100°K. Different models of the surface may exhibit midnight and cold terminator temperatures 10–20°K different, and thus one may be able to discriminate among models of the thermal properties a few centimeters beneath the surface by means of these measurements alone. Eclipse cooling curves yield information of the surface material parameters to
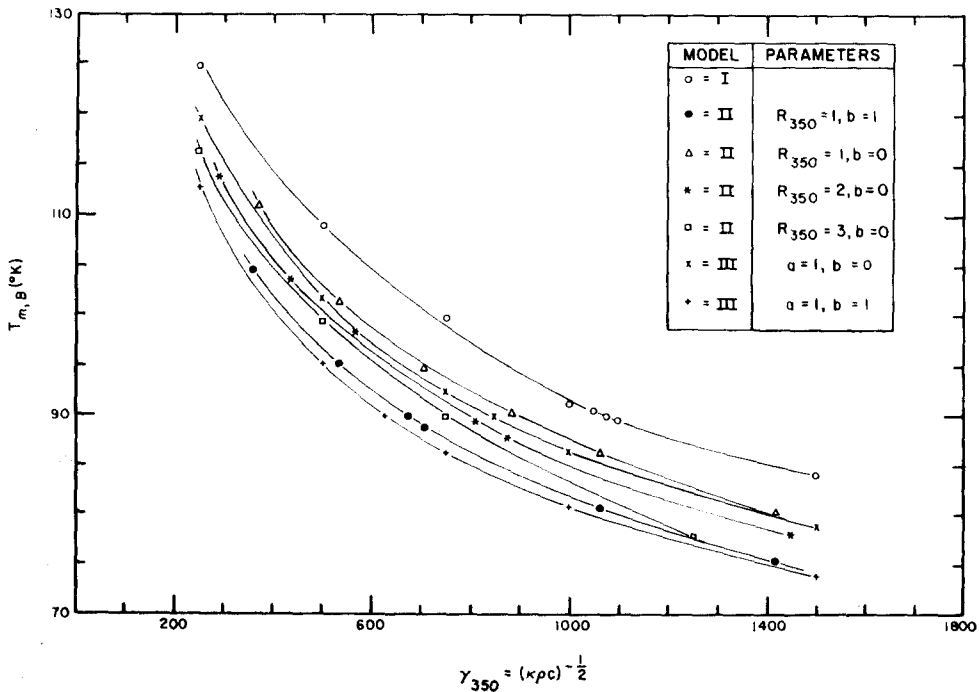


FIG. 4. The minimum surface brightness temperature at the sunrise terminator on the lunar equator as a function of $\gamma_{350}$ for the models under consideration.

TABLE IV
INFRARED COMPUTED DATA

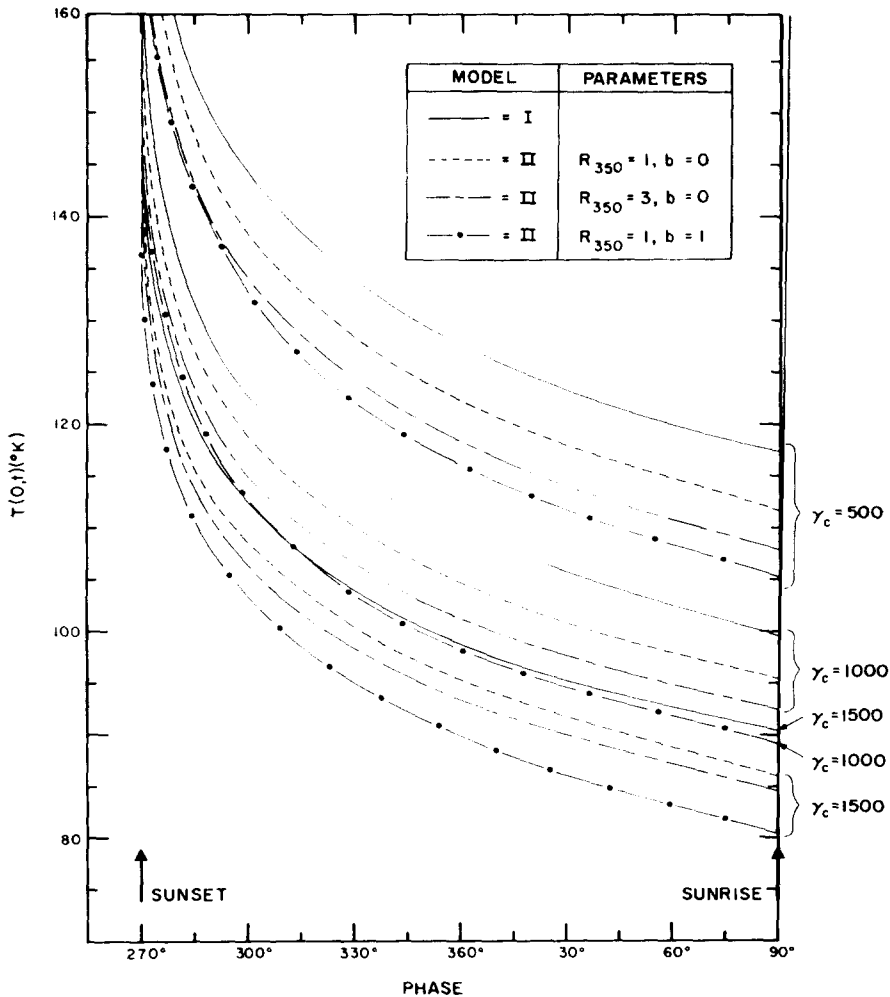| Model parameters | $s$ (mm) | $\Delta T$ (for $\langle F \rangle = 0$) (°K) | $T_0(0)$ (°K) | $\dfrac{T_1(0)}{T_0(0)}$ | $\phi_1$ (deg) | $l_{1\phi}$ (cm) | $l_{1a}$ (cm) | $L_{IT}$ (°K) | $T_{min,B}$ (°K) | $T_{mid,B}$ (°K) | $\kappa c/\rho$ or $s_0/\rho$ (cal cm⁻¹ °K⁻¹ sec⁻¹ gm⁻¹) |
|---|---|---|---|---|---|---|---|---|---|---|---|
| I $\gamma_c = 1075$ | — | 0 | 219.2 | 1.29 | 3.41 | 4.14 | 4.15 | 4.15 | 89.7 | 98.1 | $4.33 \times 10^{-6}$ |
| I $\gamma_c = 1075$, $\gamma_c = 250(x > 30\ \text{cm})$ ($F = 4.8 \times 10^{-6}$ cal cm⁻² sec⁻¹) | — | 0 | 219.4 | 1.30 | 3.41 | 4.15 | 4.20 | 4.17 | 90.2 | 98.5 | $4.33 \times 10^{-6}$ $3.46 \times 10^{-5}$ |
| II $\gamma_{350} = 885$, $\gamma_c = 1250$, $R = 1$, $b = 0$ | 0.16 | 24.0 | 219.2 | 1.29 | 3.38 | 4.17 | 4.33 | 4.25 | 90.0 | 98.3 | $3.20 \times 10^{-6}$ |
| II $\gamma_{350} = 810$, $\gamma_c = 1400$, $R = 2$, $b = 0$ | 0.25 | 38.1 | 218.7 | 1.29 | 3.32 | 4.33 | 4.10 | 4.22 | 89.5 | 97.2 | $2.55 \times 10^{-6}$ |
| II $\gamma_{350} = 750$, $\gamma_c = 1500$, $R = 3$, $b = 0$ | 0.32 | 46.5 | 219.2 | 1.30 | 3.35 | 4.59 | 4.22 | 4.41 | 90.1 | 98.3 | $2.22 \times 10^{-6}$ |
| II $\gamma_{350} = 670$, $\gamma_c = 950$, $R = 1$, $b = 1$ | 0.27 | 26.1 | 219.6 | 1.30 | 3.62 | 6.66 | 6.90 | 6.78 | 89.8 | 98.7 | $5.54 \times 10^{-6}$ |
| III $\gamma_{350} = 850$, $a = 1$, $b = 0$ | — | 33.1 | 219.4 | 1.29 | 3.43 | 4.50 | 4.13 | 4.32 | 89.7 | 98.5 | $1.99 \times 10^{-8}$ |
| III $\gamma_{350} = 625$, $a = 1$, $b = 1$ | — | 33.0 | 220.1 | 1.31 | 3.73 | 7.22 | 6.67 | 6.94 | 90.3 | 99.6 | $3.63 \times 10^{-8}$ |

FIG. 5. Computed surface temperatures during the lunar night are compared for radiative (II) and non-radiative (I) models. The parameter $R_{350}$, the ratio of radiative to conductive flux at 350°K, is a measure of the importance of radiative energy transport in these models. Phase 360° corresponds to the antisubsolar point.

smaller depths, but lunar daytime infrared measurements offer no information on these properties, since the insolation almost completely controls the surface temperature.

Recently Watson (1964) has been unable to interpret adequately the infrared scans across the evening terminator and into the lunar night obtained by Murray and Wildey (1964). His models included radiative conductivity and assumed a homogeneous stratified medium. I also have had difficulties in interpreting these data due in part to the complex nature of the observed thermal emission near the evening terminator. When observations are obtained with a finite angular resolution over a region where the surface temperature and, therefore, the emitted flux is a rapidly varying function of position, and where shadowing and small-scale inhomogeneities at the very surface play an important role, they do not readily lend themselves to an unambiguous interpretation by means of simple models. On the other hand, when one observes the thermal emission before local sunrise, none of these complications arises.
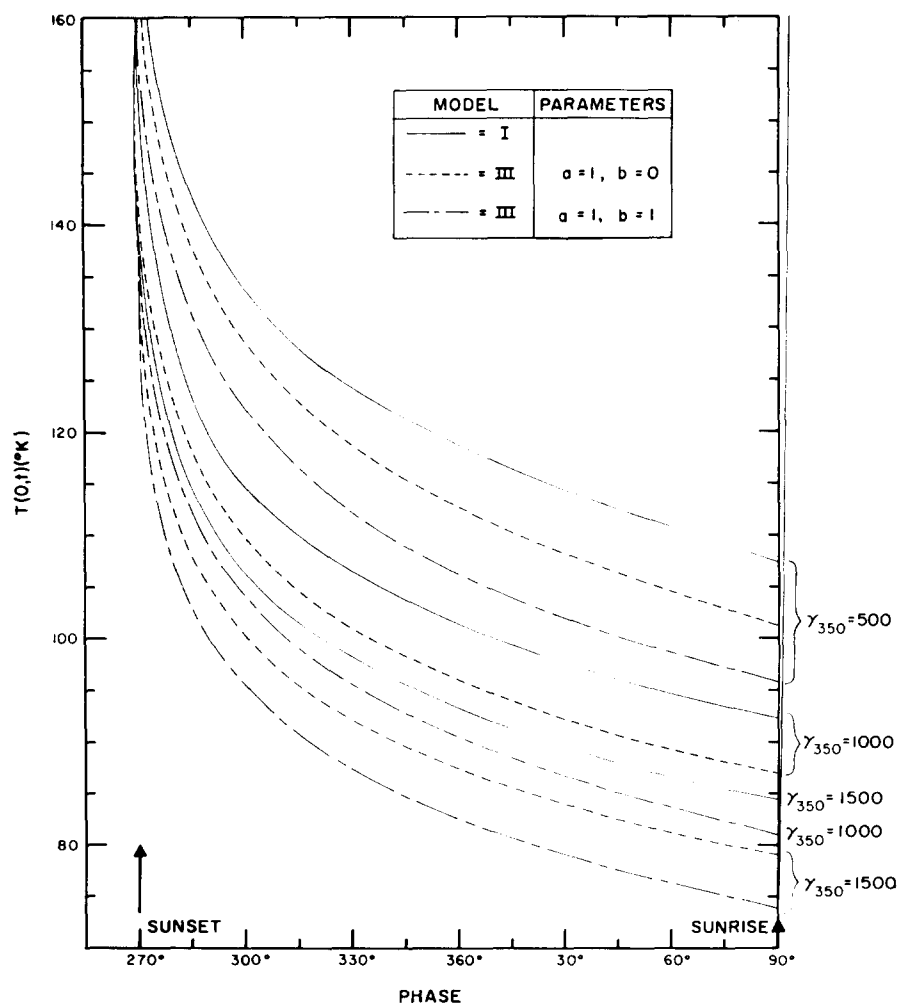
FIG. 6. Computed surface temperatures during the lunar night are compared for temperature-independent models (I) and models (III) in which the thermal conductivity and specific heat are proportional to the powers $a$ and $b$, respectively, of the temperature.

For these reasons I will use as my primary source of information infrared data on the minimum temperature reached during the lunar night, and choose those models of the surface that are in basic agreement with these data, for comparison with infrared and radio measurements.

The only infrared data available with a signal-to-noise ratio sufficient to measure the coldest lunar temperatures are those of Low (1965). He obtained a mean temperature of 90°K for the cold limb, but observed cold areas of $\leq$70°K and hot areas including one $>$150°K. Radio emission also varies from place to place, as Gary (1965) has recently confirmed, but the variation is much less. Taking 90°K to be representative for the surface brightness temperature minimum $T_{m,B}$ and in particular the value for the subterrestrial point, I have calculated models with a range of thermal parameters that are consistent with this measurement.

In Fig. 4 calculated cold limb brightness temperatures are presented as a function of $\gamma_{350}$ for the model types considered. These brightness temperatures, as mentioned above, are computed for $\epsilon_{IR} = 0.88$ and the 8–14 $\mu$ atmospheric window, but will vary
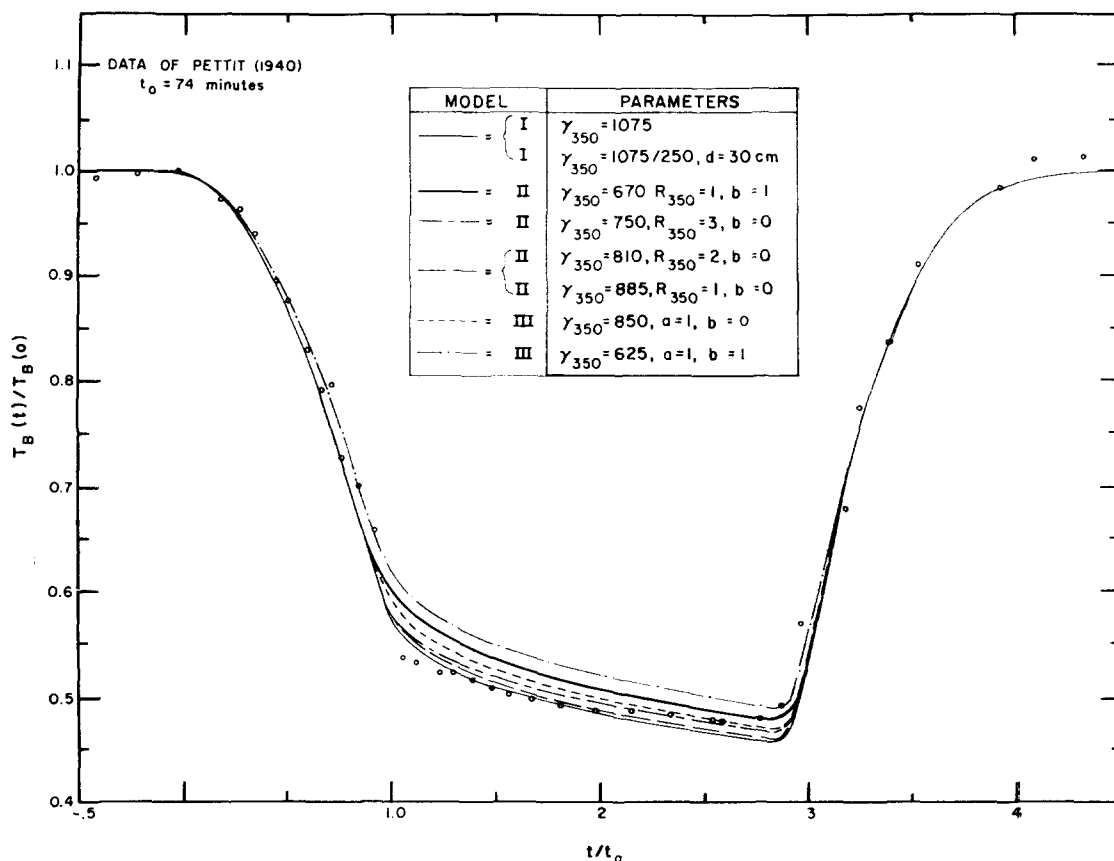
Fig. 7. Theoretical eclipse cooling curves are compared with the data of Pettit (1940) for the October 27, 1939 eclipse and lunar rectangular coordinates ($\xi = 0.$, $\eta = +0.17$). For this eclipse the duration of penumbral phase $t_0 = 74$ min, and the duration of umbral eclipse is 139 min or 1.88 $t_0$.

only by a few tenths of 1°K for observations in the 17.5–22 $\mu$ window. The models described in Table IV, representing a wide range of parameters, are consistent with this 90°K criterion. The dependence of brightness temperature upon phase during a lunation differs at most by 4°K at each terminator among the models, and, therefore, does not allow for a distinction among them from infrared measurements alone. In Figs. 5 and 6 the variation of surface temperature $T(0,t)$ with phase is presented for a representative sample of temperature-independent models to show the quantitative effect of the nonlinearities.

During the course of an eclipse, the most relevant information is obtained in the umbral phase when the conductivity and specific heat of the lunar material control

the cooling rate. One can minimize, but not eliminate, the effects of an unknown surface emissivity by considering the ratio of observed temperatures to the measured pre-eclipse temperature (see Ingrao, Young, and Linsky, 1965). This approach also minimizes errors introduced by comparing observed temperatures at positions other than the subsolar point with computations made at the subsolar point. Beyond 30° in latitude or longitude from the subsolar point, these errors computed in Ingrao, Young, and Linsky (1965) become important.

In Fig. 7 a comparison is made between the measurements of Pettit (1940) and cooling curves for the eight models computed for the circumstances of the 1939 eclipse and for the area of the lunar surface observed. None of the models fits exactly but, on the

other hand, a better representation could be achieved only by a two-layer model with a very thin upper layer and a lower layer with $\gamma_{350}$ somewhat less than 1000. Another possibility would be a composite model with several materials on the surface. Either of these situations may indeed be the case.

## VII. AN INTERPRETATION OF RADIO OBSERVATIONS

The relationship between observed brightness temperature at radio wavelengths integrated over the lunar disk $\bar{T}_R(\lambda)$ and the temperature at each depth, longitude, latitude, and time $T(x,\phi,\psi,t)$ has been discussed in the literature (see Krotikov and Troitsky, 1963 for full references). To review, one can write $T(x,\phi,\psi,t)$ assuming temperature- and depth-independent thermal properties in the form of a Fourier series

$$T(x,\phi,\psi,t) = T_0(\psi) + \sum_{n=1}^{\infty} (-1)^{a_n} T_n(\psi)$$

$$\times \exp\left[-x\left(\frac{nP}{2\alpha}\right)^{1/2}\right]$$

$$\times \cos\left(n\Phi - n\phi - \phi_n - x\left(\frac{nP}{2\alpha}\right)^{1/2}\right), \quad (32)$$

and therefore the thermal radio brightness temperature at $(\phi,\psi)$ as

$$T_R(\lambda,\phi,\psi,t) = [1 - R(\phi,\psi)]$$

$$\times \int_0^{\infty} T(x,\phi,\psi,t) k_\lambda \sec r$$

$$\times \exp(-xk_\lambda \sec r \, dx), \quad (33)$$

$$= [1 - R(\phi,\psi)]\left\{ T_0(\psi) \right.$$

$$+ \sum_{n=1}^{\infty} \frac{(-1)^{a_n} T_n(\psi)}{(1 + 2\delta_n \cos r + 2\delta_n \cos^2 r)^{1/2}}$$

$$\left. \times \cos[n\Phi - n\phi - \phi_n - \xi_n(\phi,\psi)]\right\}. \quad (34)$$

The notation is that of Krotikov and Troitsky (1963) with slight modifications and has the meaning

$T_0(\psi)$, $T_n(\psi)$, Fourier components of the surface temperature;

$\phi_n$, phase shift relative to insolation for the

$n$th Fourier component of the surface temperature;

$P$, lunar synodic period;

$\delta_n = nP/(2\alpha)^{1/2}$, ratio of the thermal attenuation coefficient for the $n$th Fourier component to the electromagnetic attenuation coefficient;

$\alpha$, diffusivity;

$a_n = (n-1)(n-2)/2$;

$R(\phi,\psi)$, surface reflection coefficient;

$\Phi = 2\pi t/P$;

$r$, angle between the normal to the surface and the direction at the point of reception; and

$\xi(\phi,\psi) = \tan^{-1}[\delta_n \cos r/(1 + \delta_n \cos r)]$, phase shift relative to insolation for the $n$th Fourier component of the radio brightness temperature.

Very often the antenna pattern integrates over a large part of the lunar disk or the whole disk, in which case the integrated thermal emission will be given by $\bar{T}_R(\lambda)$

$$\bar{T}_R(\lambda) = (1 - R_\perp)\beta_0 T_0(0)$$

$$+ (1 - R_\perp) \sum_{n=1}^{\infty} \frac{(-1)^{a_n} T_n(0)\beta_n}{(1 + 2\delta_n + 2\delta_n^2)^{1/2}}, \quad (35)$$

where the coefficients $\beta_0$ and $\beta_n$, which depend upon the dielectric constant $\epsilon$, the antenna pattern, and the observing wavelength $\lambda$, have been calculated for the case of a single-lobe antenna beam by Krotikov (1965).

In their summary paper Krotikov and Troitsky (1963) give strong arguments for a homogeneous surface layer at least to a depth of $3l_{1T}$, which is 15–20 cm for the models this analysis suggests, based upon measurements of the phase lags and amplitudes of the Fourier coefficients obtained at a number of wavelengths. These data have been interpreted by Troitsky (1962b) to show

$$\delta_1 = 2\lambda. \quad (36)$$

In addition, three independent arguments are given for a thermal parameter $\gamma_c \approx 350$ characterizing the surface material of temperature-independent properties. The first argument given is that the infrared midnight temperature $T_{mid,B}(0)$ measured by Sinton (1960) is $122° \pm 3°K$ which is consistent

with $350 < \gamma_c < 430$. This measurement was obtained by use of a pyrometer of unspecified characteristics and differs by a factor of 50 in flux from a $100°K$ antisubsolar point temperature corresponding to the cold limb data of Low (1965). Sinton's temperature is also in disagreement with the data of Saari (1964) and Low (1964).

Secondly, a value of $250 < \gamma_c < 450$ is consistent with the absolute measurements of the average brightness temperature at 3.2 cm of $211° \pm 2°K$. In contradiction to infrared measurements, these radio determinations of the temperature exhibit the same errors as flux measurements, and the "artificial Moon" calibration is subject to errors as cited above. A decrease of this measured temperature by only $5°K$ would lead to $\gamma_c = 1000$.

The final argument is based on an empirical relation between the ratio of the mean to first harmonic amplitude of the radio brightness temperature and the observed wavelength. This ratio $M = \bar{T}_{R0}/\bar{T}_{R1}$, strictly speaking, is of quantities integrated over the disk, but is nearly equal to the ratio at the center of the disk,

$$M \simeq T_{R0}(0)/T_{R1}(0).$$

The observed data have been extrapolated to $\lambda = 0$ leading to a ratio of the surface temperature Fourier components $T_0(0)/T_1(0) = 1.5$, and the relation $\delta_1 = 2\lambda$. However, the data may also be fitted equally well by the parameters

$$\left.\begin{array}{l} T_0(0)/T_1(0) = 1.3 \\ \qquad\qquad \delta_1 = 2.4 \end{array}\right\}$$

or

$$\left.\begin{array}{l} T_0(0)/T_1(0) = 1.2 \\ \qquad\qquad \delta_1 = 2.6 \end{array}\right\}.$$

Any one of a number of such parameters will also agree with the data presented. But the value of $\gamma_c$ for a homogeneous temperature-independent model varies rapidly with $T_0(0)/T_1(0)$, as shown in Table V. Therefore, this method of interpreting radio observations gives very little unambiguous information concerning the thermal properties of lunar surface materials.

In short, the value of $\gamma_c = 350\% \pm 20\%$

as given by Krotikov and Troitsky (1963) is based upon a dubious infrared measurement, an absolute radio brightness temperature for which small errors greatly affect the conclusions, and an extrapolation procedure that gives ambiguous results.

TABLE V

HOMOGENEOUS TEMPERATURE-INDEPENDENT MODELS

| $T_0(0)/T_1(0)$ | $\gamma_c$ |
|---|---|
| 1.5 | 400 |
| 1.4 | 600 |
| 1.3 | 900 |
| 1.2 | 1500 |

However, certain features of their analysis may be valid despite their conclusions, and even if the assumption of temperature-independent thermal properties is invalid, those relations will be valid for which appropriate mean quantities can be suitably defined when the heat-conduction equation is considered in its nonlinear form, Eq. (5).

One can rewrite Eq. (32) at the subsolar point $(\phi = 0, \psi = 0)$ for the more general case in the form

$$T(x,t) = T_0(x) + \sum_{n=1}^{\infty} T_n \exp\left(\frac{-x}{U_n(T)}\right)$$
$$\times \cos\left\{n\omega t - \phi_n - \frac{x}{V_n(T)}\right\}, \quad (37)$$

where $U_n(T)$ and $V_n(T)$ are analogous to a thermal wavelength but will in general not be equal. Since $U_n(T)$ and $V_n(T)$ are, in general, related to the temperature in a nonlinear manner and the mean value of the temperature $T_0(x)$ depends upon depth, these attenuation and phase-lag distance scales also depend upon depth.

At each depth considered in the lunar surface and for each computed model, a one-term Fourier series was fitted to the computed temperatures

$$T(x,t) = T_0(x) + T_1(x) \cos[\omega t - \phi_1(x)].$$
$$(38)$$

and the parameters $T_1(x)$ and $\phi_1(x)$ have been plotted in Figs. 8 and 9. Although this procedure is not, strictly speaking, a method
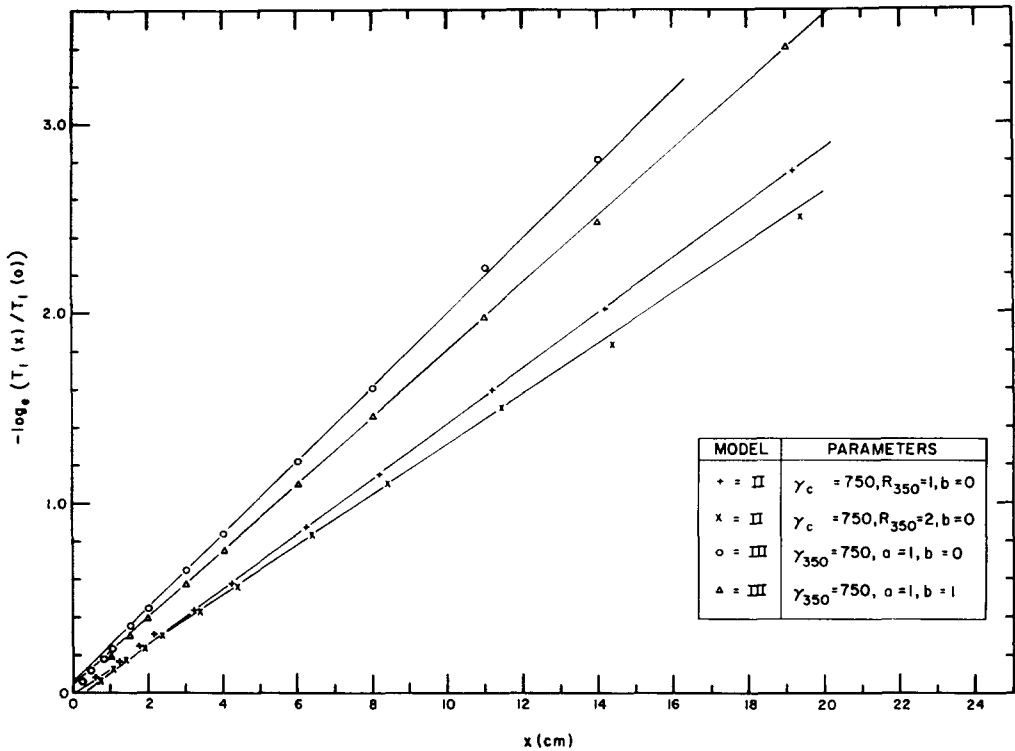
FIG. 8. Values of the first harmonic amplitudes of the computed temperature distribution obtained by a least-squares procedure at a number of depths beneath the surface are compared with the surface amplitudes for a number of models. In each case an exponential decrease with depth is an excellent approximation, so that one can define a thermal attenuation wavelength $l_{1a}$ unambiguously as that depth at which the first harmonic amplitude decreases to $e^{-1}$ of its surface value.

of solving for $U_1(T)$ and $V_1(T)$ independently, the fact that $-\log_e [T_1(x)/T_1(0)]$ and $\phi_n(x)$ obey a linear relation with depth to a very good approximation implies that $U_1$ and $V_1$ may be considered depth-independent at these depths. Beyond these depths temperature fluctuations become negligible. One can define an attenuation wavelength as that depth at which

$$- \log_e [T_1(l_{1a})/T_1(0)] = 1,$$

and a phase-lag wavelength as that depth at which

$$\Phi_1(l_{1\phi}) - \phi_1(0) = 1 \text{ radian.}$$

These quantities are listed in Table IV. In each case they differ by less than 5%, so that one can consider their average to be the effective thermal wavelength $L_{1T}$. A similar procedure could be applied to their higher

harmonics. Equation (37) can now be written as

$$T(x,t) = T_0(x) + \sum_{n=1}^{\infty} T_n \exp\left(\frac{-x}{L_{nT}}\right)$$

$$\times \cos\left(n\omega t - \phi_n - \frac{x}{L_{nT}}\right). \quad (39)$$

From this, one can derive the same equations for $\bar{T}_R(\lambda,\phi,\psi,t)$, $T_R(\lambda,0,0,t)$, and $\bar{T}_R(\lambda)$ as before except that now

$$\delta_1(\lambda) = 1/L_{1T}k_\lambda. \quad (40)$$

In Table IV there is also given the ratio of mean surface temperature to amplitude of the first harmonic for those models corresponding to a cold limb brightness temperature of 90°K. Each of the eight models under consideration exhibits a ratio very
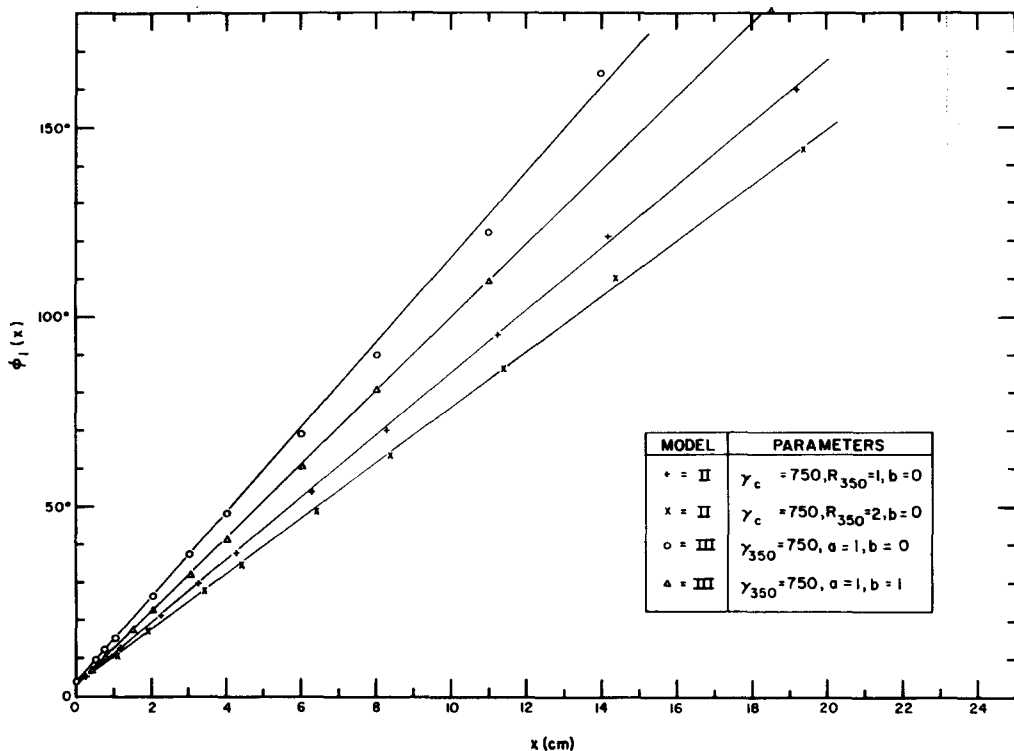
FIG. 9. Values of the first harmonic phase lags relative to surface insolation of the computed temperature distribution obtained by a least-squares procedure at a number of depths beneath the surface are compared for a number of models. In each case a linear increase with depth is an excellent approximation, so that one can define a thermal phase lag wavelength $l_{1\phi}$ unambiguous as that depth at which the first amplitude phase lag relative to insolation increases by one radian relative to the surface phase lag.

close to 1.30. From this ratio and the set of possible parameters that are in agreement with experimental amplitude ratio $M = \bar{T}_{R0}/\bar{T}_{R1}$ versus $\lambda$, we must conclude that

$$\delta_1(\lambda) = 2.4\lambda \qquad (41)$$

instead of $2\lambda$.

Computations have been made of the radio brightness temperature at the sub-terrestrial point during a lunation and an eclipse assuming

$$k_\lambda = 1/2.4\lambda L_{1T}, \qquad (42)$$

and the computed values of $L_{1T}$ listed in Table IV for a number of wavelengths and the eight surface models under consideration. These computations apply, strictly speaking, only to the center of the lunar disk and should be compared with data obtained with a resolution of better than 6' to minimize smearing of relevant detail.

Krotikov (1965) presents correction factors to be applied to the measured Fourier amplitudes and phase lags for an antenna pattern with a central lobe of Gaussian shape and arbitrary width, but no side lobes. These factors were computed for an assumed homogeneous temperature-independent surface model. Both of these assumptions may not be valid. Levin (1964) has noted that observations with low angular resolution may give a false picture of the true nature of the lunar surface material in any one region. In addition, significant variations in the radio emission have been noted over the surface at 3.3, 4, and 8.6 mm. For these reasons, I have chosen for comparison the high angular resolution data of Low and Davidson (1965) at 1–1.4 mm, Gary, Stacey, and Drake (1965) at 3.3 mm, Kislyakov and Salomonovich (1963) at 4 mm, Salomonovich and Losovsky (1962) at 8 mm, Koshchenko,

DATA OF LOW AND DAVIDSON ( 1965 )
● 3.'9 BEAM WIDTH
✦ 1.'0 BEAM WIDTH

1.2 mm

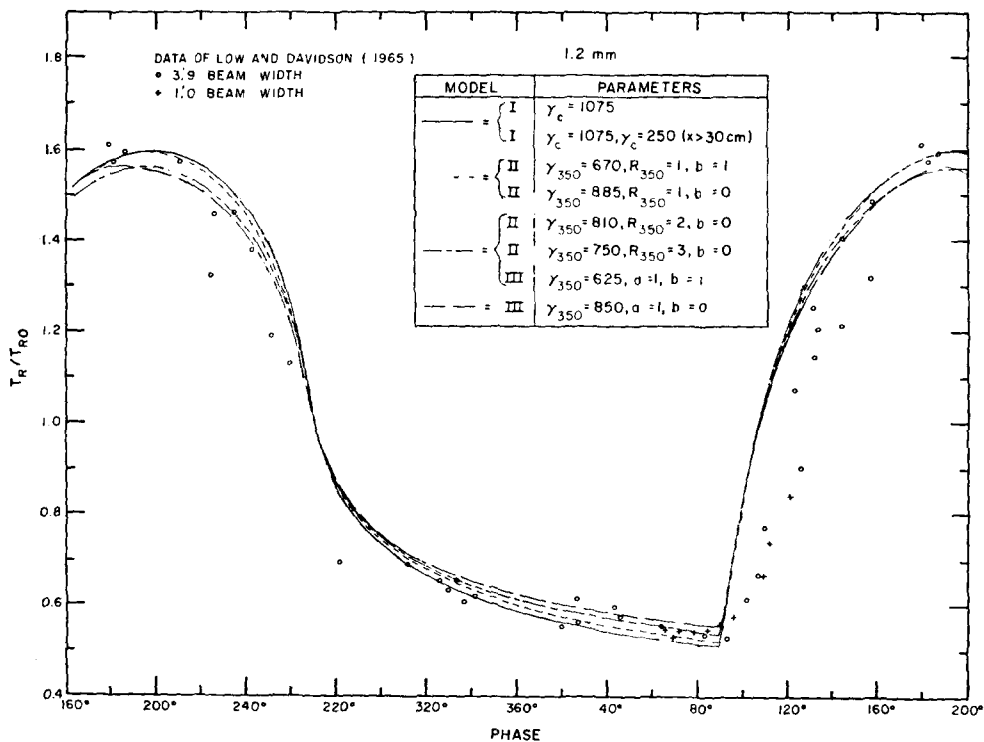| MODEL | | PARAMETERS |
|---|---|---|
| ─── = | I | $\gamma_c = 1075$ |
| | I | $\gamma_c = 1075, \gamma_c = 250 \ (x > 30 \, cm)$ |
| ─ ─ ─ = | II | $\gamma_{350} = 670, R_{350} = 1, b = 1$ |
| | II | $\gamma_{350} = 885, R_{350} = 1, b = 0$ |
| | II | $\gamma_{350} = 810, R_{350} = 2, b = 0$ |
| ─ · ─ · = | II | $\gamma_{350} = 750, R_{350} = 3, b = 0$ |
| | III | $\gamma_{350} = 625, a = 1, b = 1$ |
| ─ ─ = | III | $\gamma_{350} = 850, a = 1, b = 0$ |

$T_R/T_{RO}$

PHASE

FIG. 10. Computed radio brightness temperatures at 1.2 mm for the center of the disk are compared with the data of Low and Davidson (1965). The discrepancy between the theoretical curves and the data at the sunrise terminator ($\Phi = 90°$) may be due to shadowing by the rough surface.

DATA OF GARY, STACEY, AND DRAKE (1965)
BEAM WIDTH 2'.9

3.3 mm

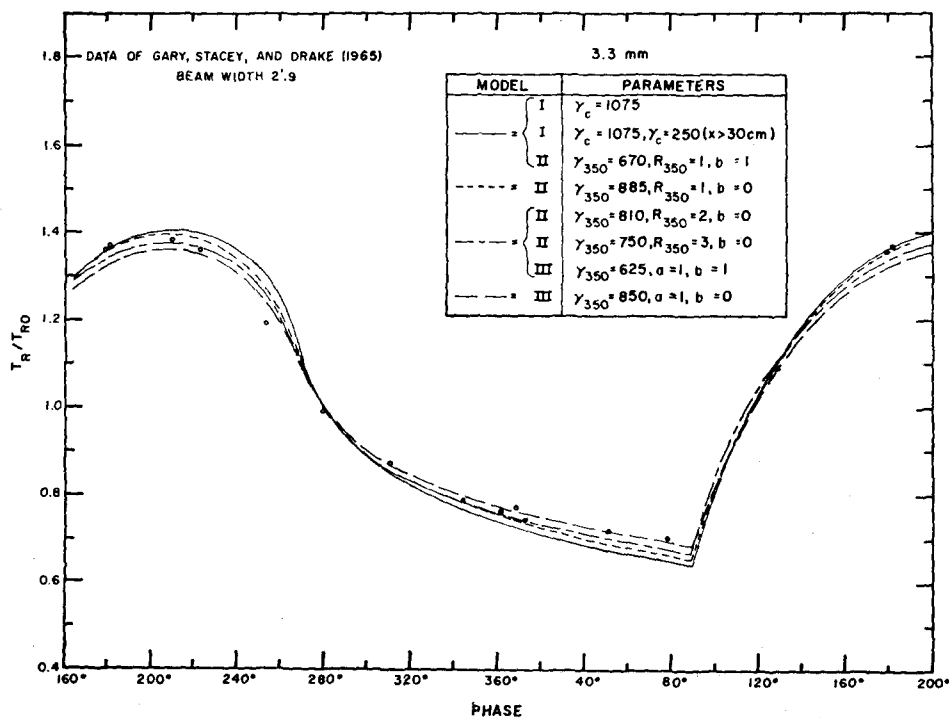| MODEL | | PARAMETERS |
|---|---|---|
| | I | $\gamma_c = 1075$ |
| ─── = | I | $\gamma_c = 1075, \gamma_c = 250 (x > 30 \, cm)$ |
| | II | $\gamma_{350} = 670, R_{350} = 1, b = 1$ |
| ─ ─ ─ ─ = | II | $\gamma_{350} = 885, R_{350} = 1, b = 0$ |
| | II | $\gamma_{350} = 810, R_{350} = 2, b = 0$ |
| ─ · ─ · = | II | $\gamma_{350} = 750, R_{350} = 3, b = 0$ |
| | III | $\gamma_{350} = 625, a = 1, b = 1$ |
| ─ ─ · = | III | $\gamma_{350} = 850, a = 1, b = 0$ |

$T_R/T_{RO}$

PHASE

FIG. 11. Computed radio brightness temperatures at 3.3 mm for the center of the disk are compared with temperatures interpolated from the isotherms of Gary, Stacey, and Drake (1965).
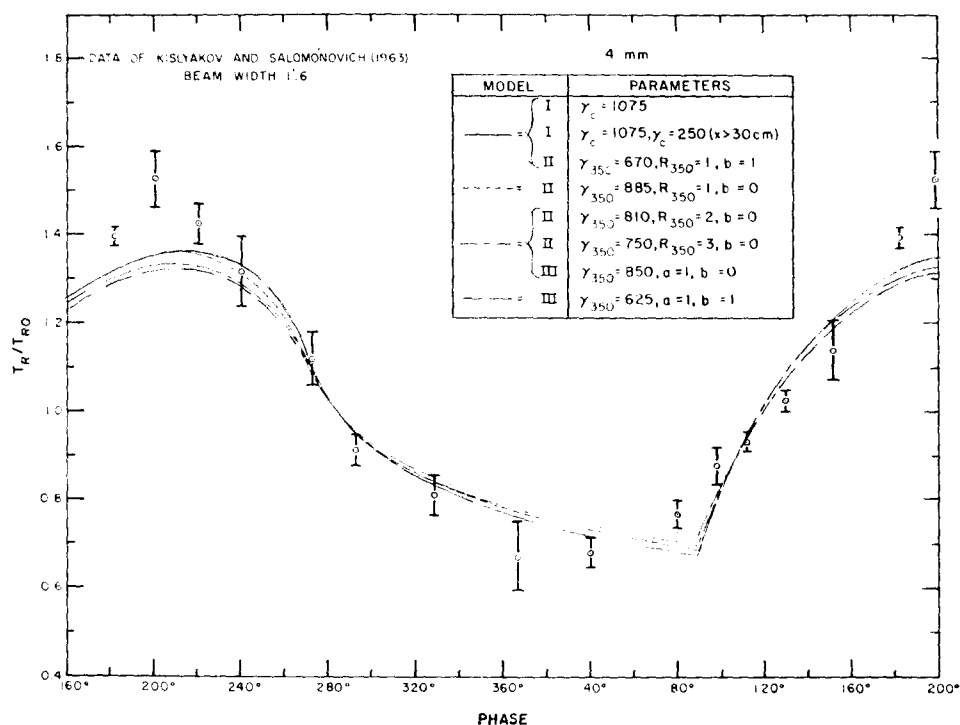
FIG. 12. Computed radio brightness temperature at 4 mm for the center of the disk are compared with the data of Kislyakov and Salomonovich (1963).

Losovsky, and Salomonovich (1961) at 3.2 cm, and Mayer, McCullough, and Sloanaker (1961) also at 3.2 cm. In each case the data, which apply to the center of the disk, have been renormalized so that the observed and computed mean temperatures agree. By this procedure I am comparing observed and computed relative temperatures that are unaffected by systematic errors and errors in the assumed surface reflectivity. The 1.2, 3.3, and 4 mm data may not be readily characterized by a one-term Fourier series and are presented along with the eight models in Figs. 10, 11 and 12.

At each wavelength there is good agreement between computations for each model and the data. The main exception to this is the 1.2 mm data at the sunrise terminator. This discrepancy can be attributed to the fact that shadowing effects are important at solar elevation angles below 20°. Mean slopes on the order of 10–12° on the scale of 1 meter have been predicted by Rea, Hetherington, and Mifflin (1964) based on radar back-scattering measurements.

In Table II the computed relative amplitudes $T_{R1}(\lambda)$ and phase lags $\phi_1(\lambda)$ for the first term of a Fourier series are compared with the data at 4 and 8 mm and 3.2 cm. The good agreement at millimeter wavelengths and at 3.2 cm suggests that each of the eight models may be representative of a large part of the lunar surface, but it in no way discriminates among them.

Lunar thermal emission has been observed during a lunar eclipse most recently at a variety of millimeter wavelengths by Kamenskaya et al. (1965), at 1–1.4 mm by Low and Davidson (1965), and at 0.8 and 1.5 mm by Baldock et al. (1965).

Unfortunately, only the data of Low and Davidson and the 1.2 mm data of Kamenskaya et al. were obtained with suitable angular resolution, 3'.9 and ~1', respectively, and under suitable observing conditions so that they could be reasonably interpreted in terms of the computed radiation emitted by a small area on the lunar surface.
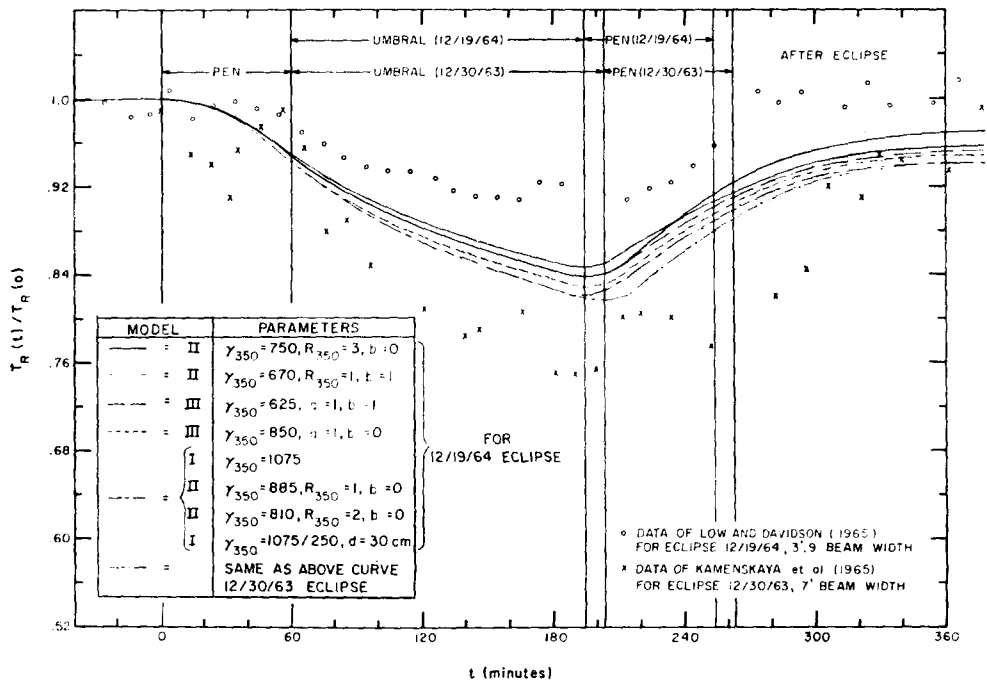
These data as shown in Fig. 13 disagree

FIG. 13. Computed radio brightness temperatures for 1.2 mm at the center of the disk for the total lunar eclipses of December 30, 1963 and December 19, 1964 are compared with the data of Low and Davidson (1965) and Kamenskaya *et al.* (1965). The circumstances of these eclipses are sufficiently similar that the two sets of data should agree.

significantly with each other and with predictions of all the models. One may therefore conclude nothing from them at this time.

## IX. CONCLUSIONS

Infrared and radio measurements can at best give information about the gross nature of the thermal properties of the lunar surface to a depth of a few tens of centimeters. Each type of data sheds light more or less unambiguously upon some aspect of the problem, but any proposed model of the lunar surface must be in agreement with all of the data.

The logical starting point of this analysis was the typical minimum temperature of 90°K for the cold terminator. Eight models of the lunar surface were proposed, including a wide range of temperature-dependent and -independent properties, characterized by $625 < \gamma_{350} < 1075$. A computer program was written to solve the heat-conduction equation for an eclipse and a lunation as well as to compute radio and infrared bright-

ness temperatures for any region of the lunar disk. This program may, with no modification, be applied to similar bodies such as Mars and Mercury or may find application in considering heat transfer for time-dependent insolation problems such as the decay of a comet.

Each of these eight models is in agreement with infrared and radio data at high angular resolution on the lunar disk. However, each model predicts a significantly different mean radio brightness temperature dependence on wavelength. To the extent that the intrinsically difficult precision measurements obtained in the USSR are free from systematic errors that depend on wavelength, two models including significant radiative energy transfer during the lunar daytime appear to be the most plausible.

These two models suggest radiative scale lengths of 0.16 and 0.27 mm, respectively, for a dielectric constant of 2.5, or 0.08 and 0.11 mm, respectively, for a dielectric constant of 1.5. Under the assumption of an

opaque material in the infrared, these scale lengths are representative of particle sizes. On the other hand, if the material is partly transparent in the infrared, which is likely for particle sizes on the order of or smaller than a wavelength, these scale lengths may be interpreted as infrared photon mean free paths. In either case one would expect a porous or grainy medium. This deduction is supported by the radar depolarization measurements of Hagfors *et al.* (1965), which suggest a tenuous surface layer at least 20 cm in depth. Hopfield's (1966) interpretation of visual negative polarization at small lunar phase angles suggests particle sizes of 5–10 $\mu$. This range of sizes may not be in conflict with that obtained above, since small particles are efficient polarizers whereas large particles and separations enhance radiative transfer. Lunar surface materials could thus consist of a wide range of particle sizes.

A porous surface material does not necessarily imply a covering of "dust" or a surface shattered by meteoric impact and covered by debris. If large regions of the lunar surface consist of uncovered lava flows, as Kuiper (1965) suggests, it is plausible to assume the physical nature of the lunar surface material is that produced by an originally molten material that upwelled and solidified in a vacuum. Recent laboratory experiments by Dobar, Tiffany, and Gnaedinger (1965) have verified that a porous medium is produced when molten silica is allowed to upwell in a vacuum. This material is of low density, reproduces lunar photometric curves, and discolors when irradiated under conditions simulating the solar wind.

The agreement between independent infrared, radio, radar, photometric measurements, and laboratory data suggests that the models presented here may be representative on a gross scale of much of the lunar surface.

### ACKNOWLEDGMENTS

### REFERENCES

ALLEN, C. W. (1963). "Astrophysical Quantities." Athlone Press, London.

BALDOCK, R. V., BOSTIN, J. A., CLEGG, P. E., EMERY, R., GAITSKELL, J. N., AND GEAR, A. E. (1965). Lunar eclipse observations at 1 mm wavelength. *Astrophys. J.* **141**, 1289.

BERNETT, E. C., WOOD, H. L., JAFFE, L. D., AND MARTENS, H. E. (1963). Properties of a simulated lunar material in air and in vacuum. *Am. Inst. Aeronaut. Astronaut. J.* **1**, 1402.

BUETTNER, K. J. K. (1963). The Moon's first decimeter. *Planetary Space Sci.* **11**, 135.

BURNS, E. A., AND LYON, R. J. P. (1963). Paper presented at the Lunar Surface Materials Conference in Boston.

BURNS, E. A., AND LYON, R. J. P. (1962). Errors in the measurement of the temperature of the Moon. *Nature* **196**, 463.

CARSLAW, H. S., AND JAEGER, J. C. (1959). "Conduction of Heat in Solids." The University Press, Oxford, England.

DOBAR, W. I., TIFFANY, O. L., AND GNAEDINGER, J. P. (1964). Simulated extrusive magma solidification in vacuum. *Icarus* **3**, 323.

EVANS, J. V., AND PETTENGILL, G. H. (1963). The scattering behavior of the moon at wavelengths of 3.6, 68, and 784 centimeters. *J. Geophys. Res.* **68**, 423.

FEDOSEYEV, L. N. (1963). Lunar and solar emission at 1.3 mm wavelength. *Radiofizika* **6**, 655.

GARY, B. (1965). Results of a radiometric Moon mapping investigation at 3 millimeters wavelength. Jet Propulsion Laboratory, in press.

GARY, B., STACEY, J., AND DRAKE, F. D. (1965). Radiometric mapping of the Moon at 3 millimeters wavelength. *Astrophys. J. Suppl. Ser.* **12**, 239.

GEOFFRION, A. R., KORNER, M., AND SINTON, W. M. (1960). Isothermal contours of the Moon. *Lowell Obs. Bull.* **5**, 1.

GOLDSMITH, A., WATERMAN, T., AND HIRSCHHORN, H. (1958). "Thermophysical Properties of Solid Materials." WADC Tech. Rept. 58-476, Armour Research Foundation.

HAGFORS, T., BROCKELMAN, R. A., DANFORTH, H. H., HANSON, L. B., AND HYDE, G. M. (1965). Tenuous surface layer on the Moon: Evidence derived from radar observations. *Science* **150**, 1153.

HAPKE, B., AND VAN HORN, H. (1963). Photometric studies of complex surfaces, with applications to the Moon. *J. Geophys. Res.* **68**, 4545.

HARRIS, D. L. (1961). Photometry and calorimetry of planets and satellites. *In* "Planets and Satellites" (G. Kuiper and B. M. Middlehurst, eds.), Chap. 8, pp. 272–342. Univ. of Chicago Press, Chicago, Illinois.

HOPFIELD, J. J. (1966). Mechanism of lunar polarization. *Science* **151**, 1380.

INGRAO, H. C., YOUNG, A. T., AND LINSKY, J. L. (1965). "A Critical Analysis of Lunar Temperature Measurements in the Infrared." Harvard College Observatory Scientific Report No. 6, NASA Research Grant No. NsG 64-60.

JAEGER, J. C. (1959). Subsurface temperatures on the Moon. *Nature* **183**, 1316.

JAEGER, J. C. (1953). Surface temperature of the Moon. *Australian J. Phys.* **6**, 10.

JAEGER, J. C., AND HARPER, A. F. A. (1950). Nature of the surface of the Moon. *Nature* **166**, 1026.

KAMENSKAYA, S. A., KISLYAKOV, A. G., KROTIKOV, V. D., *et al.* (1965). Observations of the radio eclipse of the Moon at millimeter waves. *Radiofizika* **8**, 219.

KASHENKO, V., LOSOVSKY, B., AND SALOMONOVICH, A. (1961). *Radiofizika* **4**, 425.

KISLYAKOV, A. G., AND SALOMONOVICH, A. E. (1963). Radiation of equatorial region of the Moon in 4 mm band. *Radiofizika* **6**, 431.

KROTIKOV, V. D. (1965). Averaging effect of antenna radiation pattern in measurements of radio emission of the Moon. *Radiofizika* **8**, 453.

KROTIKOV, V. D., AND SHCHUKO, O. B. (1963). The heat balance of the lunar surface layer during a lunation. *Soviet Astronomy-AJ. (Engl. Transl.)* **7**, 228.

KROTIKOV, V. D., PORFIRIEV, V. A., AND TROITSKY, V. S. (1961). *Radiofizika* **4**, 1004.

KROTIKOV, V. D., AND TROITSKY, V. S. (1963). Radio emission and nature of the Moon. *Soviet Phys.—Usp. (Engl. Transl.)* **6**, 841.

KROTIKOV, V. D., AND TROITSKY, V. S. (1964). Detecting heat flow from the interior of the Moon. *Soviet Astron.—AJ. (Engl. Transl.)* **7**, 822.

KUIPER, G. (1965). Interpretation of Ranger VII records. *Jet Propulsion Lab., Calif. Inst. Technol., Tech. Rept.* No. 32-700, Part II, Chap. 3.

LAUNER, P. (1952). *Am. Mineralogist* **37**, 764.

LEVIN, B. YU. (1964). Nature of the lunar surface layer. *Soviet Astron.—AJ. (Engl. Transl.)* **7**, 818.

LEVIN, B. YU., AND MAEVA, S. V. (1961). Some calculations of the thermal history of the Moon. *Soviet Phys.—Doklady (Engl. Transl.)* **5**, 643.

LINSKY, J. L. (1965). "A Computer Program to Solve the Heat-Conduction Equation in the Lunar Surface for Temperature-Dependent Thermal Properties." Harvard College Observatory Scientific Report No. 7, NASA Research Grant No. NsG 64-60.

LOW, F. J. (1964). Lunar observations at $\lambda 10\mu$ and 1.2 mm. *Astron. J.* **69**, 143.

LOW, F. J. (1965). Lunar nighttime temperatures measured at 20 microns. *Astrophys. J.* **142**, 806.

LOW, F. J., AND DAVIDSON, A. W. (1965). Lunar observations at a wavelength of 1 mm. *Astrophys. J.* **142**, 1278.

MAYER, C. H., McCULLOUGH, T. P., AND SLOANAKER, R. M. (1961). Measurements cited in radio emission of the Moon and planets. *In* "Planets and Satellites" (G. Kuiper and B. Middlehurst, eds.), Chap. 12, pp. 442–468. Univ. of Chicago Press, Chicago, Illinois.

MacDONALD, G. J. F. (1959). Calculations on the thermal history of the Earth. *J. Geophys. Res.* **64**, 1967.

MUNCEY, R. W. (1958). Calculations of lunar temperatures. *Nature* **181**, 1458.

MUNCEY, R. W. (1963). Properties of the lunar surface as revealed by thermal radiation. *Australian J. of Phys.* **16**, 24.

MURRAY, B. C., AND WILDEY, R. L. (1964). Surface temperature variations during the lunar nighttime. *Astrophys. J.* **139**, 734.

PETTIT, E. (1940). Radiation measurements on the eclipsed Moon. *Astrophys. J.* **91**, 408.

PETTIT, E., AND NICHOLSON, S. B. (1930). Lunar radiation and temperatures. *Astrophys. J.* **71**, 102.

PIDDINGTON, J. H., AND MINNET, H. C. (1949). Microwave thermal radiation from the Moon. *Australian J. Sci. Res., Series A*, **2**, 63.

REA, O. G., HETHERINGTON, N., AND MIFFLIN, R. (1964). The analysis of radar echoes from the Moon. *J. Geophys. Res.* **69**, 5217.

SAARI, J. M. (1964). The surface temperature of the antisolar point of the Moon. *Icarus* **3**, 161.

SALOMONOVICH, A. E., AND LOSOVSKY, B. Y. (1962). Radio-brightness distribution on the lunar disk at 0.8 cm. *Soviet Astron.—AJ (Engl. Transl.)* **6**, 833.

SINTON, W. M. (1962). Temperatures on the lunar surface. *In* "Physics and Astronomy of the Moon" (Z. Kopal, ed.). Academic Press, New York.

TOLBERT, C. W., AND COATES, G. T. (1963). "Lunar Radiation at 3.2 Millimeters and a Lunar

Model." Univ. of Texas Report 7-24. Austin, Texas.

TROITSKY, V. S. (1962a) Effect of the internal flow of heat of the Moon on its radio emission. *Radiofizika* **5**, 602.

TROITSKY, V. S. (1962b). Nature and physical state of the surface layer of the Moon. *Soviet Astron. —AJ. Engl. Transl.*) **6**, 51.

TSEYTLIN, N. M. (1963). To the method of the precise measurements by means of "the artificial Moon." *Radiofizika* **6**, 1265.

TSEYTLIN, N. M. (1964). To the measurement of antenna parameters by the radio emission of a "black" disk being in the Fresnel region. *Radiofizika* **7**, 571.

TYLER, W. C. (1961). "The Experimental Measurement and Theoretical Interpretation of Thermal Radiation from the Lunar Surface." Thesis, Univ. of Alabama, University, Alabama.

TYLER, W. C., AND COPELAND, J. (1962). A theoretical model for the lunar surface. *Astron. J.* **67**, 122.

VAN TASSEL, R. A., AND SIMON, I. (1964). Thermal emission characteristics of mineral dusts. *In* "The Lunar Surface Layer, Materials and Characteristics" (J. W. Salisbury and P. E. Glaser, eds.), pp. 445–468. Academic Press, New York.

WATSON, K. (1964). "I. Thermal Conductivity Measurements of Selected Silicate Powders in Vacuum from 150–350°K. II. An Interpretation of the Moon's Eclipse and Lunation Cooling Curve as Observed through the Earth's Atmosphere from 8–14 Microns." Thesis, California Institute of Technology, Pasadena.

WECHSLER, A. E., AND GLASER, P. E. (1965). Pressure effects on postulated lunar materials. *Icarus* **4**, 335.

WESSELINK, A. J. (1948). Heat conductivity and the nature of the lunar surface material. *Bull. Astron. Inst. Neth.* **10**, 351.